Journal of Medicinal Chemistry

Article

pubs.acs.org/jmc

Discovery of the First *C*-Nucleoside HCV Polymerase Inhibitor (GS-6620) with Demonstrated Antiviral Response in HCV Infected Patients

Aesop Cho,* Lijun Zhang, Jie Xu, Rick Lee, Thomas Butler, Sammy Metobo, Vangelis Aktoudianakis, Willard Lew, Hong Ye, Michael Clarke, Edward Doerffler, Daniel Byun, Ting Wang, Darius Babusis, Anne C. Carey, Polina German, Dorothea Sauer, Weidong Zhong, Stephen Rossi, Martijn Fenaux, John G. McHutchison, Jason Perry, Joy Feng, Adrian S. Ray, and Choung U. Kim

Gilead Sciences, 333 Lakeside Drive, Foster City, California 94044, United States

Supporting Information

ABSTRACT: Hepatitis C virus (HCV) infection presents an unmet medical need requiring more effective treatment options. Nucleoside inhibitors (NI) of HCV polymerase (NS5B) have demonstrated pan-genotypic activity and durable antiviral response in the clinic, and they are likely to become a key component of future treatment regimens. NI candidates that have entered clinical development thus far have all been *N*-nucleoside derivatives. Herein, we report the discovery of a *C*-nucleoside class of NS5B inhibitors. Exploration of adenosine analogs in this class identified 1′-cyano-2′-*C*-methyl 4-aza-7,9-dideaza adenosine as a potent and selective inhibitor of NS5B. A monophosphate prodrug approach afforded a series of compounds showing submicromolar activity in HCV replicon assays. Further pharmacokinetic optimization for sufficient oral absorption and liver triphosphate loading led to identification of a clinical development candidate GS-6620. In a phase I clinical study, the potential for potent activity was demonstrated but with high intra- and interpatient pharmacokinetic and pharmacodynamic variability.

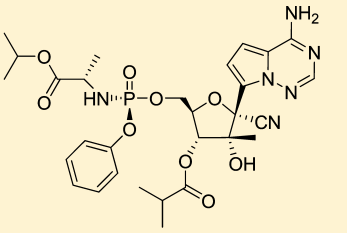

HCV GT1-6 replicons EC_{50} = 68 - 427 nM

INTRODUCTION

Hepatitis C virus (HCV) infection presents a global heath problem in need of more effective treatment options. The World Health Organization estimates that 130−170 million individuals have detectable antibodies to HCV worldwide, corresponding to 3% of the world's population. Approximately 60−85% of such cases develop into chronic disease, leading to liver cirrhosis (5−25%), end-stage liver disease, and hepatocellular carcinoma (1−3%) over the course of the disease.[1] The current standard of care (SOC) includes administration of pegylated interferon-α (Peg-IFN) and ribavirin (RBV), which primarily relies on the patient's ability to build up an immune response against the virus. However, this SOC is suboptimal in that it affords variable efficacy across the multiple genotypes of HCV as well as poor safety and tolerability.[2] Recently, there has been an intense thrust for development of small molecule therapeutic agents directly targeting the viral replication and infectivity.[3] The HCV genome (9.6 kb single (+)-strand RNA) encodes both structural and nonstructural proteins (NS2 to NS5), most of which have been exploited as drug targets. These drug discovery efforts resulted in a number of direct-acting antivirals (DAAs) entering clinical development over the past several years. In 2011, two DAAs (NS3 protease inhibitors; teleprevir and boceprevir) were approved for clinical use in combination with Peg-IFN/RBV. Although these regimens substantially improve response rates, they are limited to the treatment of HCV genotype 1 infected patients, and they suffer from the combined side effects of both Peg-IFN/RBV and the new drugs themselves.[4] Therefore, there is still an urgent need for interferon-sparing regimens consisting of multiple DAAs for higher efficacy and improved tolerability.[5]

A number of DAAs targeting various viral essential proteins have demonstrated antiviral response in HCV infected patients.[3] Among them, nucleoside inhibitors (NIs) of NS5B polymerase have a profile that suggests they will be critical components in future treatment regimens.[6] Class related properties that differentiate NI from other classes of HCV inhibitors include a high genetic barrier to drug resistance, allowing for durable antiviral suppression, and pan-genotype anti-HCV activity affording universal treatment coverage. However, the complex nature of the nucleoside pharmacology poses a great difficulty in predicting efficacy and safety in humans, resulting in high attrition during drug development.

Several nucleoside polymerase inhibitors have entered clinical trials. Recent examples are shown in Figure 1.[7,8] Structurally, all of these compounds are *N*-nucleosides containing a 2′-*C*-Me branched sugar. Some of the 2′-*C*-Me *N*-nucleosides were synthesized as early as the late 1960s prior to the discovery of HCV, but their in vitro anti-HCV activity was not discovered until the early 2000s.[9,10] These inhibitors are metabolized in cells to their respective nucleoside

Special Issue: HCV Therapies

Received: February 7, 2013

dx.doi.org/10.1021/jm400201a | *J. Med. Chem.* XXXX, XXX, XXX−XXX

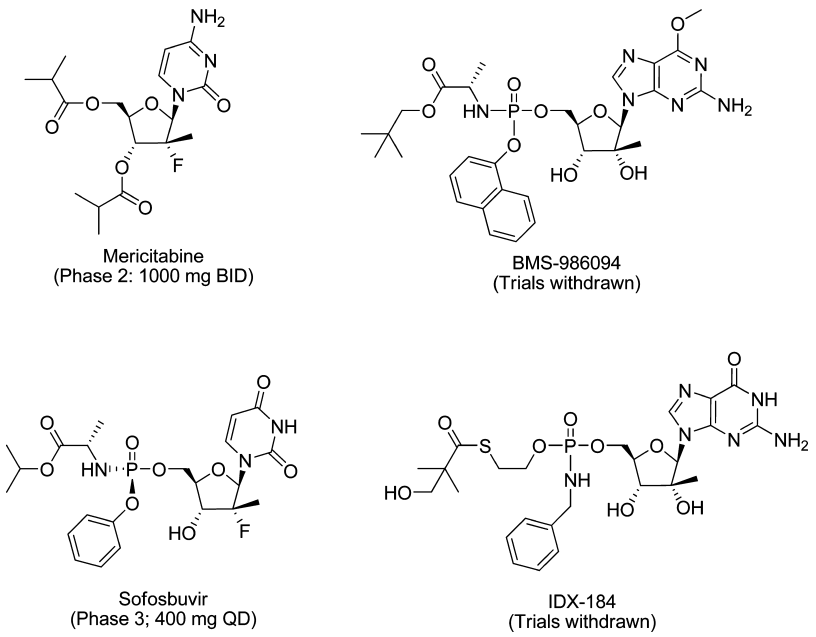

Figure 1. Nucleoside polymerase inhibitors and their clinical development status[7,8].

triphosphates, which bind to the active site of the NS5B polymerase as a substrate and become incorporated into a growing chain of viral RNA. Upon incorporation, they inhibit further RNA elongation, resulting in inhibition of viral replication. The 2′-*C*-Me group prevents an incoming nucleoside triphosphate from binding to the active site of NS5B.[11]

Previously, we reported the synthesis and structure−activity relationship (SAR) of *C*-nucleosides containing the 2′-*C*-Me group as NS5B inhibitors.[12] In this earlier study, 2′-*C*-methyl 4-aza-7,9-dideaza adenosine (**1**) was identified as a selective inhibitor of HCV replication in cell cultures (EC_{50}(1b) 1.98 μM, Table 1). Compound **1** can be viewed as a *C*-nucleoside variant of an *N*-nucleoside 2′-*C*-methyl-7-deaza adenosine **29** (MK-608), which was one of the most potent adenosine analogs reported in the literature at the time we initiated this work.[13] Compared to **29**, the replicon activity of **1** was rather weak (EC_{50} 0.08 μM for **29**) despite its triphosphate being as potent as the **29** triphosphate at inhibiting NS5B-mediated RNA synthesis in an enzyme assay (IC_{50} 0.31 μM for **1**, 0.30 μM for **29**). This discrepancy was explained by a difference in efficiency of triphosphate formation in replicon cells (Huh-7). Compound **1** was metabolized to its biologically active triphosphate species less efficiently than **29** in Huh-7 cells. While less efficiently metabolized in Huh-7 cells, **1** was actually more efficiently metabolized in primary hepatocytes in vitro and more efficient at forming its active triphosphate in liver following oral administration to rodents than **29**. The combined similar intrinsic potency and improved hepatic delivery suggest that **1** would exhibit potent in vivo anti-HCV activity rivaling that observed for **29**.[14]

Table 1. Comparison of *N*-Nucleoside and *C*-Nucleoside 7-Deazaadenosine Analogs[a]

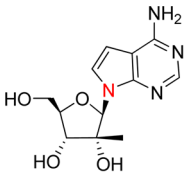

29 (MK-608)

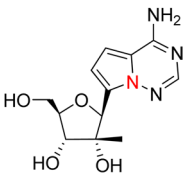

1

	29	**1**
EC_{50} (1b, μM)	0.08	1.98
CC_{50} (Huh-7, μM)	>89	85
IC_{50} as NTP (1b, μM)	0.30	0.31
NTP level (C_{max}, pmol/million)		
in Huh-7 cells	25	5
in human hepatocytes	8	22

[a]Summary of results reported previously.[12]

In the hopes of improving the cellular selectivity of **1**, we have pursued further structural modifications on both the base and the sugar moieties. Previously, we also reported a series of 1′-substituted *C*-nucleosides displaying antiviral activity against various RNA viruses, including HCV.[15] Thus, we decided to incorporate the 1′-substitution into **1**. This strategy resulted in the identification of 1′-cyano-2′-*C*-methyl 4-aza-7,9-dideaza adenosine (**2**), which, as its triphosphate, showed a substantially improved selectivity over mitochondrial RNA polymerase (POLRMT) while maintaining the intrinsic NS5B inhibitory activity. A monophosphate prodrug approach was undertaken to achieve the whole cell replicon activity. Further pharmacokinetic optimization led to the discovery of **18** (GS-6620), the first *C*-nucleoside clinical candidate. In phase I studies, the compound demonstrated the potential for potent anti-HCV activity in HCV-infected patients, but with a high PK/PD variability.[16]

RESULTS AND DISCUSSION

On the basis of the favorable properties previously reported for **1**,[12] toxicology studies were conducted in Sprague−Dawley rats. Disappointingly, oral administration of **1** once a day for 7 days resulted in unscheduled deaths at 20 and 40 mg/(kg day). The no-observable adverse effects level (NOAEL) was determined to be less than 5 mg/(kg day), the lowest dose tested in the studies. Adverse effects included necrosis in organs such as the kidney, liver, and pancreas, as well as lymphocellular

dx.doi.org/10.1021/jm400201a | J. Med. Chem. XXXX, XXX, XXX−XXX

depletion. This toxicity profile had a resemblance to amanitin mushroom poisoning, which is primarily caused by inhibition of host mRNA synthesis by RNA polymerase II (Pol II).[17] To understand the cause for the toxicity, the triphosphate of **1** was tested against a series of host DNA and RNA polymerases. While the triphosphate did not inhibit Pol II, it was a good substrate for POLRMT. Since POLRMT is likely a key mediator of ribonucleotide analog toxicity,[18] we monitored selectivity over this off-target enzyme in our discovery program.

In light of the finding that the triphosphate of **1** was a substrate of POLRMT, a possible cause for the observed toxicity in rats, further structural modification of **1** was sought for improved selectivity. Applying chemistry that we have developed,[15] a series of 1′-substituted analogs of **1** were prepared and evaluated (Table 2). Among those tested, 1′-cyano-2′-*C*-methyl 4-aza-7,9-dideaza adenosine (**2**) was the most active as its triphosphate in the NS5B enzyme assay and, importantly, not a substrate for POLRMT. Other 1′-substituted analogs (**3**, **4**) had no appreciable NS5B inhibitory activity. Overall, an addition of the CN group at the 1′ position of **1** maintained the intrinsic enzyme activity, while abolishing the incorporation by POLRMT.

Table 2. 1′-Substituted Analogs of 1[a]

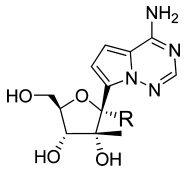

compd	R	EC_{50} (1b, μM)	IC_{50} (1b, μM)	mtRNA SNI (%)
1	H	1.98	0.31	21
2	cyano	>89	0.29	0.03
3	methyl	>89	55	0.08
4	ethynyl	>89	>200	ND

[a]See the Experimental Section for detailed assay protocols.

However, compound **2** was not active in the whole cell replicon assay. This was not surprising, since previous studies showed that the 1′-substitution limits the first of three phosphorylation steps in metabolic conversion to the biologically active nucleoside triphosphate.[15] Accordingly, a phosphoramidate-type monophosphate prodrug (**5**) was prepared and tested in the HCV replicon assay. It was found to exhibit respectable replicon activity (EC_{50} (1b) 1.05 μM). It was also shown that a high level of the triphosphate (~20 μM) was formed when 10 μM of **5** was incubated for 24 h in Huh-7 cells that host the GT1b replicon. In comparison, less than 0.5 μM of the triphosphate was detected with the incubation at 10 μM of the parent nucleoside **2**. These results indicate that the first-step phosphorylation is slow, but the second and third phosphorylations are efficient (Figure 2).

On the basis of the potent enzyme activity, the remarkable selectivity over POLRMT, and the whole cell replicon activity as the monophosphate prodrug, compound **2** became our lead nucleoside for prodrug optimization. Various monophosphate prodrug approaches have been utilized to overcome the first-step phosphorylation and enhance antiviral activity of the parent nucleosides.[19] Among them, the phosphoramidate-type prodrug approach has recently demonstrated clinical utility in the treatment of HCV infection. For example, a phosphoramidate prodrug of 2′-C-Me-2′-F-uridine (sofosbuvir) has demonstrated high sustained virologic response (SVR) rates when administered in combination with other antiviral agents for the treatment of chronic HCV infection and has advanced to phase III clinical trials.[20] A similar chemical approach was adopted in our work, initially focusing on SAR study around the

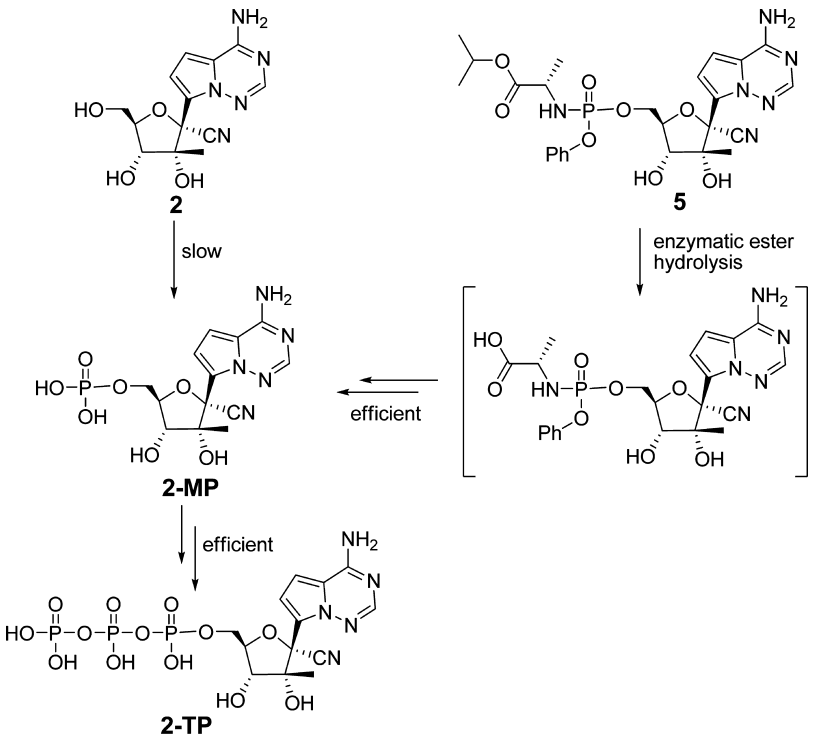

Figure 2. Monophosphate prodrug activation starts with an enzymatic ester hydrolysis, which leads to formation of the 5′-monophosphate (**2-MP**), which is further phosphorylated to the biologically active 5′-triphosphate (**2-TP**). Nucleoside **2** itself is poorly phosphorylated to **2-MP**.

dx.doi.org/10.1021/jm400201a | J. Med. Chem. XXXX, XXX, XXX–XXX

phosphoramidate portion of **5**. Since the enzymatic ester hydrolysis is known to be the first step in prodrug activation, phosphoramidate prodrugs with various ester groups were prepared and their anti-HCV activity tested (Table 3).

Table 3. HCV Replicon Activity of Phosphoramidate Prodrugs[a]

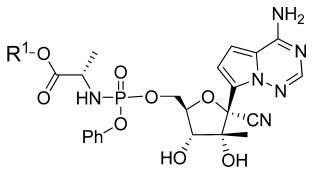

compd	R1	EC_{50} (1b, μM)	CC_{50} (Huh-7, μM)
6	Me	1.37	>89
7	Et	1.45	>89
5	*iso*-Pr	1.05	>89
8	(S)-*sec*-Bu	0.23	>89
9	(R)-*sec*-Bu	0.98	>89
10	*t*-Bu	>89	>89
11	*cyc*-pentyl	0.45	>89
12	*neo*-pentyl	0.18	85
13	2-EtBu	0.44	35
14	Bn	0.33	63

[a]See the Experimental Section for detailed assay protocols.

Prodrugs with primary and secondary alcohol esters (**5**–**9**, **11**–**14**) were all active in the replicon assay, but the tertiary alcohol ester prodrug (**10**) was inactive, presumably due to the lack of enzymatic ester hydrolysis. Bigger and more lipophilic alkyl esters generally showed higher potency; however, cytotoxicity was observed in the case of *cyclo*-pentyl (**12**), 2-ethylbutyl (**13**), and benzyl (**14**) esters.

The ultimate goal for the program was to identify an orally active agent. To be orally active, the monophosphate prodrug must be well absorbed upon oral administration and travel to the liver without degradation. The intact prodrug should then be efficiently metabolized and converted to the triphosphate in the liver, the major site for HCV replication. Thus, at the outset, we aimed at achieving both high oral absorption and efficient liver triphosphate loading. To assess the oral absorption potential for these compounds, in vitro DMPK properties relevant to oral absorption were evaluated first (Table 4). Water solubility was acceptable (>100 μg/mL) for prodrugs with alkyl esters containing less than five carbons. However, as the lipophilicity (log *D*) was increased, the solubility dropped sharply. With a couple of exceptions (**8** and **14**), Caco-2 permeability was low with high efflux potential. Intestinal absorption turned out to be a major issue with this series of prodrugs (see below for further discussion). Stability in both serum and intestinal S9 was excellent for secondary alkyl esters. On the other hand, a majority of these prodrugs were efficiently metabolized by hepatic S9, suggesting liver-specific activation. To assess the liver triphosphate loading potential, compounds were incubated in primary human hepatocytes and the resulting triphosphate levels were measured. All compounds except **10** produced high levels of triphosphate, where the relative order of the level of the triphosphate tracked well with the relative replicon activity.

To profile in vivo characteristics of these prodrugs, pharmacokinetic studies assessing liver triphosphate levels were performed in hamsters. Following intravenous (iv) and oral administrations (po), levels of the triphosphate metabolite in the liver were determined (Table 5). The iv dosing resulted

Table 5. In Vivo PK Properties of Phosphoramidate Prodrugs

	hamsters, liver triphosphate			dogs, plasma prodrug		
	C_{max} (μM)[a]		%	$AUC_{0\text{-}inf}$ (μM·h)[c]		%[d]
compd	iv	po	"oral efficiency"[b]	portal	jagular	Fa
6	6.35	0.29	0.9			
7	4.48	0.57	2.5			
5	5.65	0.53	1.9	0.99	0.16	10
8	ND	1.27		0.80	0.12	16
9	ND	1,87		0.46	0.14	8.1
11	2.80	0.84	6.0			
12	5.18	1.44	5.6	0.25	0.09	13
13	8.33	2.26	5.4	0.21	0.02	7.9
14	ND	0.86				

[a]Dosed at 1 mg-equiv/kg for iv, 5 mg-equiv/kg for po. [b]"oral efficiency" = po C_{max} ÷ 5/iv C_{max} × 100%. [c]Dosed at 0.5 mg/kg. [d]See the Experimental Section for details.

Table 4. Physicochemical Properties, Permeability and Stability in Human Extracts of Select Phosphoramidate Prodrugs[a]

			Caco-2 permeability ($\times 10^{-6}$ cm/s)[b]				
compd	log *D*	solubility (μg/mL)[c]	A to B	B to A	intestinal S9 stability ($t_{1/2}$, min)	hepatic S9 (% extraction)	TP formation in hepatocytes[d]
6	1.3	ND	0.41	4.64	190	90	+
7	1.6	108	0.17	2.98	69	89	+
5	1.8	306	0.16	8.92	>612	90	+
8	2.1	200	1.47	17.9	592	93	++
9	1.9	151	0.75	37.5	461	94	+
10	2.2	380	0.67	31.1	>612	84	NT
11	2.2	10	0.37	5.86	30	95	++
12	2.3	115	0.69	29.1	85	94	+++
13	2.7	1.8	0.36	7.20	74	97	+++
14	2.2	0.05	3.35	25.3	129	93	+++

[a]See the Experimental Section for detailed assay protocols. [b]Permeability through Caco-2 cells determined at 10 μM. [c]Measured at pH 7. [d]Relative levels of triphosphate measured upon 1 h of incubation (10 μM) with primary human hepatocytes; +++, very high (>200 pmol/million); ++, high; +, medium (50–100 pmol/million).

dx.doi.org/10.1021/jm400201a | J. Med. Chem. XXXX, XXX, XXX–XXX

in relatively high levels of the triphosphate in all cases, suggesting highly efficient liver loading. However, triphosphate levels were substantially lower following oral administration, suggesting inefficient oral absorption. The "oral efficiency" of liver triphosphate loading based on dose-normalized po triphosphate C_{max} relative to iv triphosphate C_{max} was poor (<10%). These results suggest that only a small fraction of the prodrugs were delivered to the liver by the oral route due to inefficient prodrug absorption. To gain further insight, oral absorption for selected prodrugs was determined in portal vein cannulated dogs where both absorption and hepatic extraction can be measured. In line with the poor oral delivery in hamsters, oral absorption in dogs was poor (<20%) in all cases evaluated. The in vivo results from these two different animal studies strongly suggested this class of compounds has limitations on oral bioavailability.

We then sought out other ways of improving the oral absorption potential. Strategies such as replacement of L-alanine with other L-amino acids (e.g., glycine, L-leucine, L-phenylalanine) and substitutions on the phenyl ring (e.g., 2-F, 2,4-diMe, 3,4-methylenedioxy) were explored, but they proved unfruitful. All these prodrugs, for example, suffered from poor permeability with high efflux ratio, which will be summarized in a further publication. Next, a double prodrug approach was sought where one or two hydroxyl groups of the nucleoside sugar were protected. Accordingly, compounds with 2′,3′-*O*-carbonate (**15**) and the 3′-*O*-isobutyrate (**16**) were prepared[21] and evaluated in a series of both in vitro and in vivo assays (Table 6). Remarkably, compound **16** achieved substantially higher liver triphosphate loading in hamsters compared to the 3′-unsubstitued precursor prodrug **5**, when administered orally (liver TP C_{max} 3.67 μM vs 0.53 μM). Furthermore, oral absorption in dogs for **16** was substantially high (88%). Caco-2 permeability was also substantially improved, corroborating the in vivo results (Figure 3). In particular, the efflux effect was dramatically reduced at a high incubation concentration (efflux ratio of <2 at 100 μM). In addition, **16** delivered a much higher level of the triphosphate in primary human hepatocytes. Thus, **16** achieved our targeted preclinical profile. Encouraged by these results, the liver pharmacokinetic profile in dogs was determined (Figure 4). Upon oral administration at 5 mg/kg, the triphosphate levels in the liver exceeded the IC_{90} over 24 h, suggesting the potential to be effective in treating patients infected with HCV at a reasonable dose.

Table 6. Comparison of Selected Prodrugs[a]

	5	15	16
EC_{50} (1b, μM)	1.05	1.41	0.61
CC_{50} (Huh-7, μM)	>89	>89	47
log *D*	1.8	2.6	2.9
hamsters, liver TP C_{max} (μM); iv/po	5.63/0.53	1.92/0.59	4.50/3.67
dogs, % oral absorption	10	29	88
human hepatocytes TP (C_{max}, pmol/million)	82	60	274

[a]See the Experimental Section for detailed assay protocols.

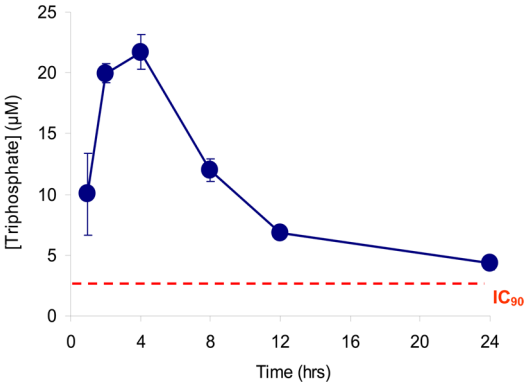

Figure 4. Mean liver versus time profile of the triphosphate metabolite following oral administration of **16** to beagle dogs (5 mg/kg; solution) (mean ± SD; n = 2/time point for dog).

Nonclinical toxicology studies were then conducted with compound **16**. Rats and dogs were dosed for 7 days at up to 300 and 75 mg/(kg day), respectively. No test-article related toxicities were observed from these studies. Consequently, the NOAEL was established at >300 mg/(kg day) for rats and >75 mg/(kg day) for dogs. The results for **16** were in striking contrast to those described earlier for the 1′-unsubstitued *C*-nucleoside **1**, establishing a correlation between the in vitro observation of incorporation by POLRMT and in vivo toxicity. Subsequent toxicology studies further established the tolerability of this nucleotide prodrug. The NOAEL values were the highest doses tested following chronic administration with **18** (a pure diastereoisomer of **16**, see below) for 26 weeks in rats and 39 weeks in dogs (1,000 and 60 mg/(kg day), respectively).

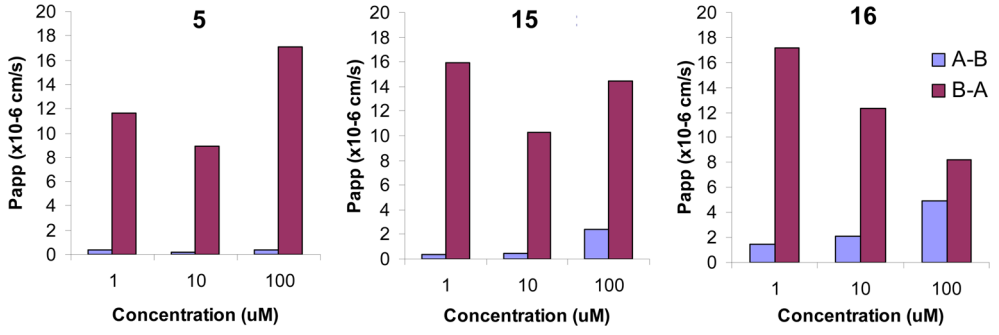

Figure 3. Prodrug **16** has high permeability and minimal efflux when tested at 100 μM in caco-2 cells. At lower concentrations, reduced forward permeability and increased efflux ratio is observed, suggesting **16** is subject to saturable efflux transport. The apical to basolateral permeability of **16** is increased 10-fold over that observed for the des-3′-isobutyryl prodrug **5**. The blue bar is for forward permeability and the red bar for backward permeability.

dx.doi.org/10.1021/jm400201a | J. Med. Chem. XXXX, XXX, XXX–XXX

Compound **16** is a diastereomeric mixture at the phosphorus center of the phosphoramidate pro-moiety. To select the optimal isomer for clinical development, the two single diastereomers (**18** and **20**) were profiled separately and their properties compared. Compared to the *Rp* isomer **20**, the *Sp* isomer **18** was 6-fold more potent in the replicon assay and two times more efficient in the triphosphate formation in primary human hepatocytes, and it achieved 3-fold higher levels of liver triphosphate following oral administration to hamsters. Thus, **18** was the preferred isomer and was selected as a clinical development candidate.

The antiviral characteristics of **18** or its diastereomeric mixture **16** were more fully assessed in studies presented in the Supporting Information. In an expanded panel of the replicon assay using stable replicons GT1b, 1a, and 2a and chimeric replicons 2b, 3a, 4a, 5a, and 6a, **18** displayed potent inhibition against all the genotypes tested with EC_{50} ranging between 0.068 μM and 0.43 μM (Table S1). These results were in contrast to those of a non-nucleoside NS5B inhibitor tested in the same assays that showed EC_{50} values varying over 600-fold depending on genotype. As observed with other 2′-*C*-Me nucleos(t)ides, such as **29** and 2′-*C*-Me adenosine, **16** had a significantly reduced activity (>95 fold) against the replicon encoding the S282T mutation in NS5B. No resistance was observed for the N142T mutation selected by the nucleoside analog 4′-azido cytidine (Table S2). Combinations of **16** with anti-HCV agents from the non-nucleoside NS5B, NS5A inhibitor, and NS3 protease inhibitor classes in an Huh-7 cell line carrying GT 1a replicon showed additive to minor synergy in antiviral activity (Table S3).

The antiviral activity, safety, and tolerability of **18** were evaluated in a randomized, double-blind, placebo controlled, multiple-dose, dose-escalation study in treatment-naïve subjects chronically infected with HCV genotype 1.[16] Nine cohorts (consisting of eight active and two placebo) assessing doses between 50 mg once daily and 900 mg twice daily (BID) administered under fed or fasted conditions for 5 days were studied. Compound **18** was demonstrated to be safe and well tolerated at up to 900 mg BID for 5 days. The greatest antiviral activity was observed in BID cohorts with median viral load reductions of 1.73 and 1.63 $\log_{10}$ IU/mL from baseline with 900 mg administered as a tablet or 450 mg administered as a solution, respectively. The potential for potent antiviral activity was evident in two patients in the 900 mg BID cohort who had their viral loads reduced to below the lower limit of quantification (representing respective viral load reductions of greater than 3.37 $\log_{10}$ IU/mL and 4.37 $\log_{10}$ IU/mL) and one patient in the 450 mg solution cohort achieving a viral load reduction of 4.06 $\log_{10}$ IU/mL. However, substantial intra- and interpatient PK/PD variability was observed in all cohorts. For example, in the 900 mg BID cohort **18**, exposure on day 5 varied by more than an order of magnitude (ranging from 41.6 ng h/mL to 760 ng h/mL) and maximal viral load reductions varied by more than 3 orders of magnitude (ranging from 1.14 $\log_{10}$ IU/mL to greater than 4.37 $\log_{10}$ IU/mL). Notably, plasma levels of **18** were markedly lower than those observed preclinically in dogs, suggesting a species difference in prodrug absorption or metabolism.

CHEMISTRY

Previously, we reported a convergent synthesis of *C*-nucleosides.[12,15,22] The key step of synthesis involves a carbon–carbon bond formation between protected ribonolactones and fully functionalized heteroaromatic bases. This reaction leads to various 1′-hydroxy *C*-nucleosides, which are versatile intermediates for a number of both 1′-unsubstituted and substituted *C*-nucleosides. Applying this chemistry, a series of 1′-substituted 2′-*C*-Me nucleosides (**2**–**4**) were prepared. For preparation of **2**, the 1′-hydroxy intermediate **21**[12] was subjected to an acid-promoted replacement of the 1′-hydroxyl group by the 1′-CN. This reaction was highly stereoselective, affording a single stereoisomer **22** as the sole isolated product. This can be explained by blockage of the β-face approach of the CN nucleophile toward the acid-induced five-membered-ring oxocarbenium ion due to steric congestion exerted by the neighboring 2′-β-Me. Subsequent debenzylation was conveniently achieved by boron trichloride (Scheme 1). Although the debenzylation reaction was clean as long as the boron reagent (1 M BCl_3 in dichloromethane) was fresh, adequate neutralization of the crude reaction mixture using a base such as sodium methoxide or triethylamine during workup was necessary to avoid unwanted hydrolysis of the 1′-CN group.

Scheme 1. [a]

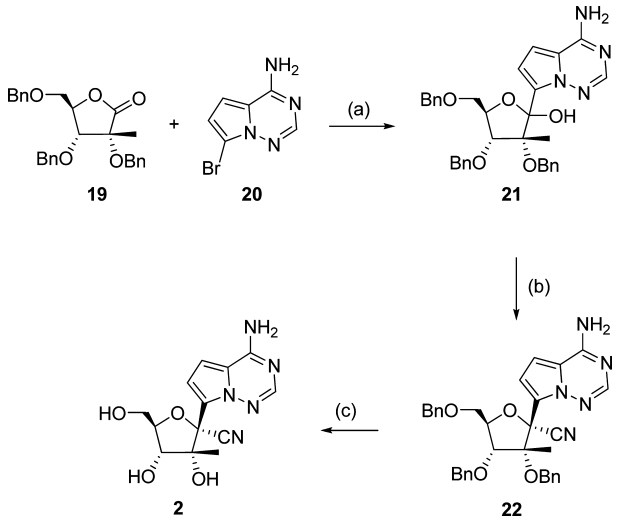

[a]Reagents and conditions: (a) **20,** 1,1,4,4-tetramethyl-1,4-dichlorodisilylethylene (1.0 equiv) and *n*-BuLi (3.3 equiv), THF, −78 °C followed by addition of **19**, 1 h, 65–80%; (b) TMSCN (6 equiv), TMSOTf (4 equiv), CH_2Cl_2, −15 to 0 °C, 2 h, 85–95%; (c) BCl_3 (3 equiv), CH_2Cl_2, 0 °C, 1 h, 90%.

A number of phosphoramidate prodrugs derived from nucleoside **2** were prepared initially following the literature methods, which conventionally afforded the products as a mixture of two diastereomers at the phosphorus center (**5**–**14**).[8,23] For example, compound **5** was prepared by reacting **2** in the presence of *N*-methylimidazole with the chloridate **24,** which was freshly prepared by treatment of L-alanine isopropyl ester with phenyl phosphorus dichloridate (Scheme 2). Trimethyl phosphate was used as a cosolvent to improve the solubility of **2** and maintain a homogeneous solution throughout completion of the reaction. Since the chloridate **25** was produced as an even mixture of the two diastereomers at the phosphorus, the subsequent reaction product **5** was also a diastereomeric mixture. Later in our program, some analogs (e.g., compounds **8** and **9**) were prepared by a modified method where the *p*-nitrophenolates as phosphorylating

dx.doi.org/10.1021/jm400201a | J. Med. Chem. XXXX, XXX, XXX–XXX

Scheme 2. [a]

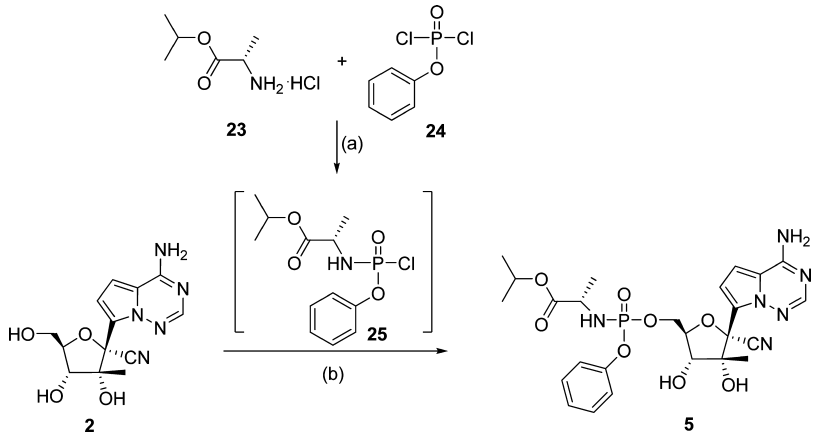

[a]Reagents and conditions: (a) triethylamine, CH_2Cl_2, −78 °C and then warm to rt, 16 h; (b) *N*-methyl imidazole, trimethyl phosphate and THF, 0 °C to rt, 2 h, overall yield 59%.

Scheme 3. [a]

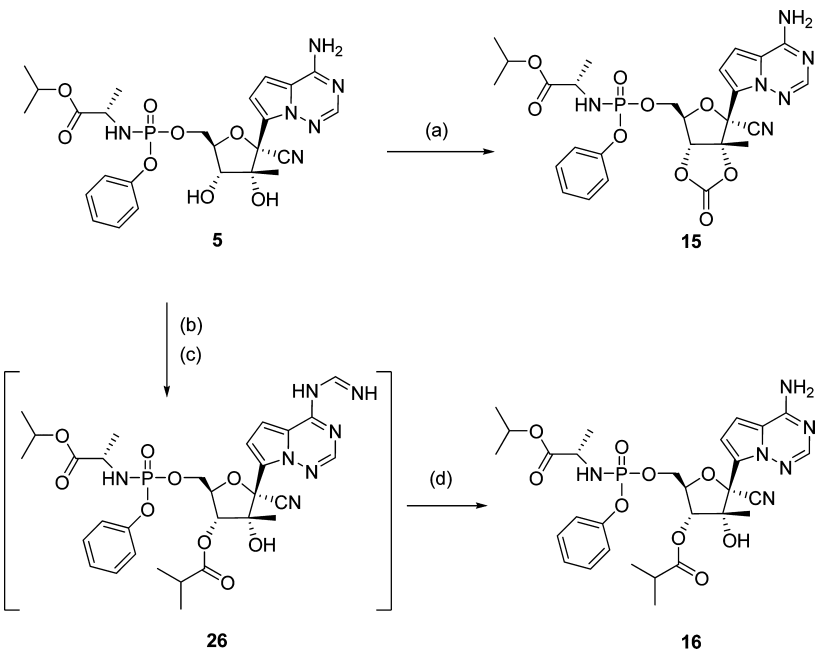

[a]Reagents and conditions: (a) CDI, CH_3CN, rt, 6 h, 86%; (b) *N,N* -dimethylformamide dimethyl acetal, CH_3CN, rt, 1 h; (c) isobutyric acid, DCC, CH_3CN, rt, 48 h; (d) water-TFA, 0 °C to rt, 64 h, overall yield 73%.

reagents and *tert*-butyl magnesium chloride as a base were used (as in Scheme 5).

For the 2′,3′-di-*O*-carbonate prodrug **15**, compound **5** was simply treated with CDI . For the 3′-O-butyrate prodrug **16**, however, protection of the 6-amino group was required. The 6-amino group of **5** was transiently protected as a formamidine using *N,N*-dimethylformamide dimethyl acetal, and then the 3′-OH was acylated by treatment of isobutyric acid and DCC. Deprotection in aqueous TFA led to **16** in high overall yield from this three-step process (Scheme 3).

Initially, the diastereomeric mixture **16** was separated by chiral column chromatography (Chiralcel OD-H; heptanes and isopropyl alcohol) to obtain the two single diastereomers (**18** and **20**). However, preparation of **18** in larger quantities required a more practical method. Thus, stereospecific synthesis using a single diastereomeric alternative to the chloridate **25** was sought. The single isomeric phosphorylating reagent should be stable, readily separable from the diastereomeric mixture, and react with a 5′-hydroxyl group of the nucleoside **2** stereospecifically to afford the phosphate ester formation. After brief screening, the *p*-nitrophenolate **28** was identified as the one that met these criteria.[24] Accordingly, the diastereomeric mixture **28** was prepared and subjected to chiral column chromatography or fractional crystallization to obtain the single isomer (*Sp*)-**28** (Scheme 4). Its absolute stereochemistry was determined by single crystal X-ray analysis (CDCD 929320). Nucleoside **2** was treated with 1.5 equiv of *tert*-butyl magnesium chloride in THF, and subsequent treatment of the resulting suspension with (*Sp*)-**28** at 50 °C for 2−3 h afforded the (*Sp*)-isomer **18** (Scheme 5), of which the absolute stereochemistry was also determined by X-ray crystallography (CDCD 929321, Figure 5).

dx.doi.org/10.1021/jm400201a | *J. Med. Chem.* XXXX, XXX, XXX−XXX

Scheme 4. [a]

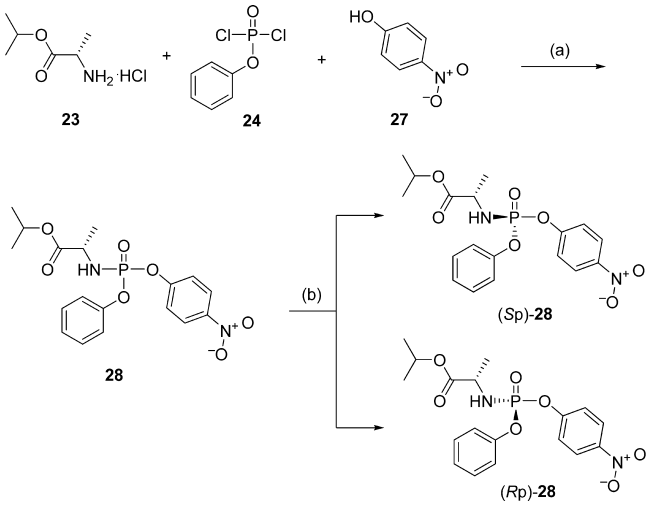

[a]Reagents and conditions: (a) triethylamine, CH_2Cl_2, −20 °C to rt, 77%; (b) Chiralpak IC, 70% heptanes and 30% isopropanol, or crystallization from diethyl ether and hexanes for (*Sp*)-**28**.

CONCLUSION

Incorporation of the cyano group at the 1′ position of the previously disclosed 2′-*C*-methyl-7-deaza adenosine *C*-nucleoside (**1**) resulted in a novel class of nucleoside **2**, which displayed the desired level of NS5B enzyme inhibitory activity and selectivity. Phosphoramidate prodrugs such as **5** afforded potent replicon activity and high triphosphate loading in vitro but suffered from low oral absorption in animals. This problem was solved by 3′-*O*-acylation. From these efforts, compound **18** was identified, becoming the first *C*-nucleoside class of NS5B inhibitors to enter clinical development. In the first-in-man studies, **18** displayed proof of concept and the potential for potent antiviral activity, but its clinical utility was limited by high PK/PD variability.

EXPERIMENTAL SECTION

Nuclear magnetic resonance (NMR) spectra were recorded on Varian Mercury Plus 400 MHz and a Varian Unity Plus 500 MHz spectrometers at room temperature, with tetramethylsilane as an internal standard. Chemical shifts (δ) are reported in parts per million (ppm), and signals are reported as s (singlet), d (doublet), t (triplet), q (quartet), m (multiplet), or br s (broad singlet). Purities of the final compounds were determined by HPLC and were greater than 95%. HPLC conditions to assess purity were as follows: Agilent HPLC, Phenominex Kinetex C18, 4.6 mm × 100 mm (2.6 μm); gradient of 0.1% FTA water (A) and 0.1% TFA acetonitrile (B); flow rate, 1.5 mL/min; acquire time, 9 min; wavelength, UV 214 and 254 nm; oven. The preparative HPLC system includes two sets of Gilson 332 pumps, a Gilson 156 UV/vis detector, and a Gilson 215 injector and fraction collector, with Trilution LC software. A Synergi 150 mm × 30 mm 4u Hydro-RP 80 A column was used. The mobile phase was a HPLC grade water (A) and HPLC grade acetonitrile (B) system. LC/MS was conducted on a Thermo Finnigan MSQ Std using electrospray both positive and negative [M + H^+ and M − H^+], and a Dionex Summit HPLC System (model: P680A HPG) equipped with a Gemini 5 u C18 110A column (30 mm × 4.60 mm), eluting with 0.05% formic acid in 1% acetonitrile/water (solvent A) and 0.05% formic acid in 99% acetonitrile/water (solvent B). High-resolution mass spectra were recorded on a Xevo G2 Q-Tof mass spectrometer with an ESI source.

2′,3′,5′-*O*-Tribenzyl-1′-hydroxy-2′-*C*-methyl-4-aza-7,9-dideazaadenosine (21). To a dry, argon purged 1 L round-bottom flask with stir bar at room temperature were charged the aryl bromide **20** (8.0 g, 38 mmol) and anhydrous THF (500 mL). The suspension was gently stirred for 10 min. At this point, 1,2-bis-(chlorodimethylsilyl)ethane (8.2 g, 38 mmol) was added as a solid, and the sides of the vessel were rinsed with a small volume of THF. Within a few minutes, the mixture became cloudy. The mixture was allowed to stir for 10 min. At this point, solid NaH (60% in mineral

Scheme 5. [a]

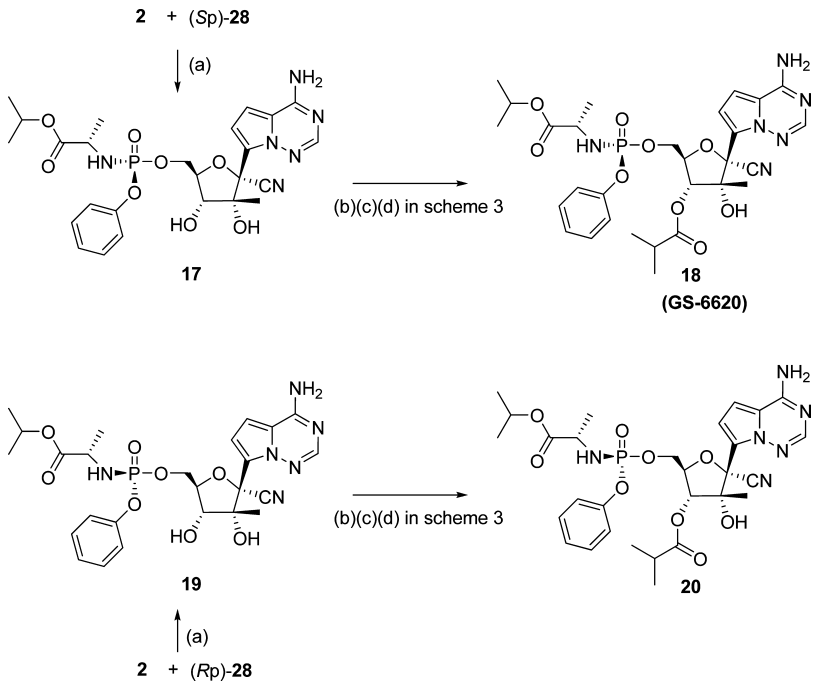

[a]Reagents and conditions: (a) **20,** *t*-BuMgCl (1.5 equiv), THF, rt, 10 min and then (*Sp*) or (*Rp*)-**28**, 50 °C, 3 h, 70−90%; (b), (c), (d) same as in Scheme 3.

dx.doi.org/10.1021/jm400201a | J. Med. Chem. XXXX, XXX, XXX−XXX

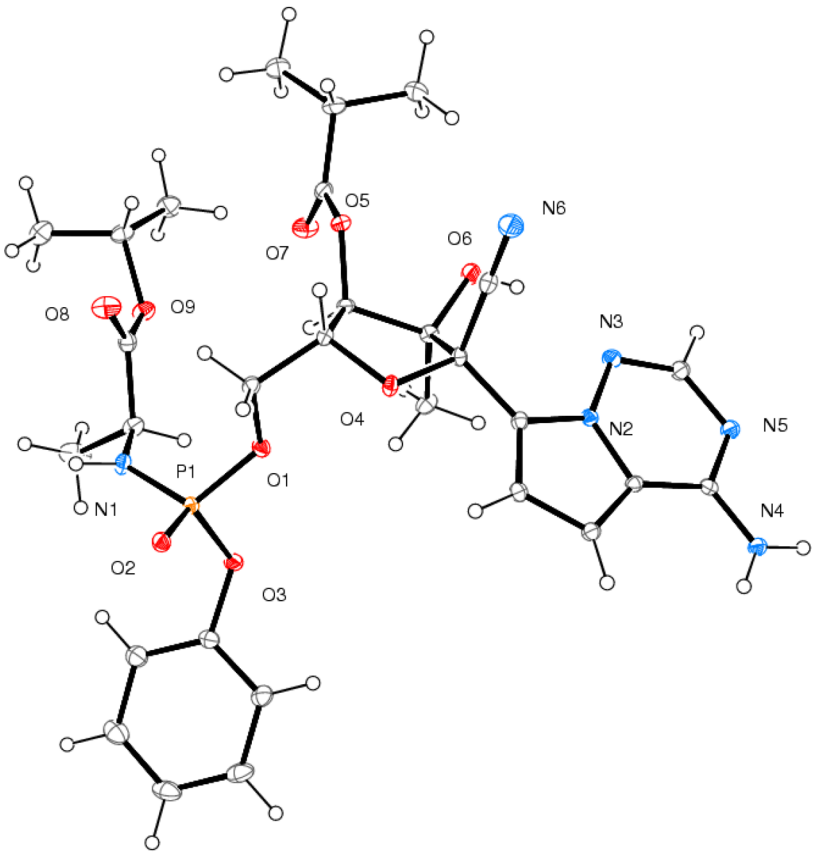

Figure 5. X-ray crystal structure of **18**.

oil; 3.8 g, 95 mmol) was added in three portions. The resulting mixture was stirred for 5 min and then cooled to −78 °C over 45 min. Separately, an oven-dried addition funnel purged with argon was charged with BuLi (1.6 M in hexanes, 78 mL, 125 mmol). Then, BuLi was added dropwise to the mixture at −78 °C over 45 min. The reaction progress was monitored by HPLC, and the starting material **20** was almost completely consumed by the time the addition was complete. Another oven-dried argon purged addition funnel was charged with a solution of the lactone **19** (19 g, 44 mmol) in anhydrous THF (~70 mL). This solution was then added dropwise to the −78 °C solution of the lithio species over 45 min and allowed to stir under argon at the same temperature for 2 h. The cold bath was removed to allow the reaction mixture to warm slightly (30 min). The cold reaction mixture was slowly poured into a large rapidly stirring flask containing 1 M citric acid (800 mL) and EtOAc (500 mL). The mixture was allowed to stir for 15 min and was transferred to a separatory funnel (2 L). The organic phase was separated. The aqueous phase was extracted with EtOAc (2 × 400 mL). The combined organic extracts were washed sequentially with water (1 × 400 mL), saturated $NaHCO_3$ (2 × 400 mL), water (1 × 400 mL), and brine (1 × 400 mL), dried over sodium sulfate, and then concentrated to dryness. The crude was purified by silica gel flash column chromatography (50% hexanes + 50% EtOAc to 100% EtOAc), affording **21** as a glassy solid obtained (17.2 g, 81%). MS, *m*/*e* 567 $(M + 1)^+$. ^1H NMR (300 MHz, $CDC1_3$) δ 7.85 (m, 1H), 7.27 (m, 15H), 7.01 (m, 1H), 6.51 (m, 1H), 4.66 (m, 8H), 4.40 (m, 2H), 3.79 (m, 3H), 1.62 (s, 2′-CH_3 from one isomer), 1.18 (s, 2′-CH_3 from the other isomer).

2′,3′,5′-*O*-Tribenzyl-1′-cyano-2′-*C*-methyl-4-aza-7,9-dideazaadenosine (22). To a solution of compound **21** (azeotropically dried using toluene, 6.8 g, 12 mmol) in CH_2Cl_2 (150 mL) at −15 °C was added TMSOTf (56 mmol) dropwise. Then TMSCN (73 mmol) was added dropwise. The reaction mixture was stirred at −15 °C for 1.5 h and warmed to 0 °C for an additional 0.5 h. The reaction was quenched with saturated $NaHCO_3$ (75 mL) at 0 °C and diluted with CH_2Cl_2 (100 mL). The organic phase was separated, washed with brine (150 mL), dried over Na_2SO_4, and concentrated. The residue was purified by silica gel column chromatography (eluted with hexanes−EtOAc 0 to 100%) to give the desired product **22** (6.9 g, 93%). MS, *m*/*e* 576 $(M + 1)^+$. ^1H NMR (300 MHz, $CDCl_3$) δ 7.98 (s, 1H), 7.2−7.5 (m, 15H), 7.11 (d, 1H), 6.63 (d, 1H), 5.78 (brs, 2H), 4.99 (ABq, 2H), 4.4−4.8 (m, 5H), 4.04 (d, 1H), 3.96 (dd, 1H), 3.75 (dd, 1H), 1.16 (s, 3H).

1′-Cyano-2′-*C*-methyl-4-aza-7,9-dideazaadenosine (2). To a solution of compound **22** (20 g, 35 mmol) in CH_2Cl_2 (200 mL) at 0 °C was added BCl_3 (105 mL, 1 M in CH_2Cl_2) over 10 min. The reaction mixture was stirred at the same temperature for 1 h. An ice-cold sodium methoxide in methanol (25%, 50 mL) was dropwise added over 3 min. The mixture was stirred at 0 °C for 30 min and then allowed to warm up to room temperature for 30 min. The mixture was concentrated, and the residue was redissolved in methanol (200 mL) and concentrated again. This process was repeated twice. The residue was dissolved in methanol. Silica gel (~30 g) was added and concentrated. The residue was purified by silica gel column (0−20% methanol/CH_2Cl_2) to give the desired product **2** (9.5 g, 90%). ^1H NMR (300 MHz, D_2O): δ 7.74 (s 1H), 6.76 (d, J = 5 Hz, 1H), 6.73 (d, J = 5 Hz, 1H), 4.1 (m, 1H), 3.9 (m, 1H), 3.8 (m, 2H), 0.84 (s, 3H). MS, *m*/*e* 306 $(M + 1)^+$. HRMS, calculated for $C_{13}H_{15}N_5O_4$ $(M + 1)^+$, 306.1197; found, 306.1203.

(2*S*)-Isopropyl 2-((((2*R*,3*R*,4*R*,5*R*)-5-(4-Aminopyrrolo[1,2-*f*][1,2,4]triazin-7-yl)-5-cyano-3,4-dihydroxy-4-methyltetrahydrofuran-2-yl)methoxy)(phenoxy)phosphorylamino)propanoate (5). Phenyl phosphorodichloridate (4.99 g, 23.8 mmol) was dissolved in dichloromethane (100 mL), and L-alanine isopropyl ester hydrochloride (3.98 g, 23.8 mmol) was added. The resulting clear solution was cooled to −78 °C over 30 min. Triethylamine (6.63 mL, 47.5 mmol) was added dropwise over 15 min. The mixture was then allowed to warm to room temperature. After 6 h, the solvent was removed under an argon stream. The residue was redissolved in MTBE (25 mL), and the insoluble portion was removed by filtration

dx.doi.org/10.1021/jm400201a | *J. Med. Chem.* XXXX, XXX, XXX−XXX

under argon. The filtrate was then condensed with an argon stream, and the crude product **25** was used for the next reaction without further purification. ^{1}H NMR (300 MHz, CDC_{13}) δ 7.1−7.4 (m, 5H), 5.1 (m, 1H), 4.35 (m, 1H), 4.15 (m, IH), 1.5 (d, 3H), 1.2 (m, 6H). ^{31}P NMR (121.4 MHz, CDC_{13}) δ 7.8, 8.4 (s).

To a solution of compound **2** (1.03 g, 3.37 mmol) in trimethyl phosphate (2.0 mL) and THF (20 mL) was added *N*-methyl imidazole (1.5 g, 18.3 mmol) at 0 °C. A solution of compound **25** (2.5 g, 8.18 mmol) in THF (3 mL) was dropwise added. The resulting mixture was allowed to warm to room temperature over 1.5 h. The mixture was partitioned between ethyl acetate and water. The ethyl acetate layer was concentrated, and the residue was purified by silica gel chromatography (ethyl acetate to 10% ethanol/ethyl acetate), affording 1.15 g (59%) of compound **5** as a 1:1 diastereomeric mixture at phosphorus. ^{1}H NMR (300 MHz, $CDC1_3$) δ 8.02 (s, 1H), 7.1−7.4 (m, 5H), 6.8 (2d, 1H), 6.7 (2d, 1H), 6.08 (brs, 2H), 5.03 (m, 1H), 4.6 (m, 1H), 4.4 (m, 2H), 3.9−4.1 (m, 3H), 1.31 (d, 3H), 1.2 (m, 6H), 0.83 (s, 3H). ^{31}P NMR (121.4 MHz, $CDC1_3$) δ 2.78 (s). MS, *m/e* 575 $(M + 1)^+$.

(2*S*)-Methyl 2-((((2*R*,3*R*,4*R*,5*R*)-5-(4-Aminopyrrolo[1,2-*f*][1,2,4]triazin-7-yl)-5-cyano-3,4-dihydroxy-4-methyltetrahydrofuran-2-yl)methoxy)(phenoxy)phosphorylamino)propanoate (6). ^{1}H NMR (300 MHz, $CDC1_3$) δ 8.98 (s, 1H), 7.1−7.3 (m, 5H), 6.75 (2d, 1H), 6.60 (2d, 1H), 5.75 (brs, 2H), 4.55 (m, 1H), 4.35 (m, 2H), 3.6−4.1 (m, 3H), 3.62 (s, 3H), 1.31 (d, 3H), 0.83 (s, 3H). MS, *m/e* 547 $(M + 1)^+$.

(2*S*)-Ethyl 2-((((2*R*,3*R*,4*R*,5*R*)-5-(4-Aminopyrrolo[1,2-*f*][1,2,4]triazin-7-yl)-5-cyano-3,4-dihydroxy-4-methyltetrahydrofuran-2-yl)methoxy)(phenoxy)phosphorylamino)propanoate (7). ^{1}H NMR (500 MHz, DMSO-d_6) δ 7.91 (s, 1H), 7.85 (brs, 2H), 7.1−7.4 (m, 5H), 6.90 (2d, 1H), 6.79 (2d, 1H), 6.11 (2dd, 1H, NH), 5.98 (s, 1H, 2′-OH), 5.45 (2d, 1H, 3′-OH), 4.41 (m, 1H, 5′-CH_2), 4.24 (m, 1H, 5′-CH_2), 4.20 (m, 1H, 4′-CH), 4.05 (m, 1H, 2H, OCH_2), 3.86 (m, 1H, NHCH), 3.70 (t, 1H, 3′-CH), 1.25 (q, 3H, $CHCH_3$), 1.14 (m, 3H, CH_2CH_3), 0.92 (s, 3H). ^{31}P NMR (202.3 MHz, DMSO-d_6) δ 3.94, 3.94 (s). MS, *m/e* 561 $(M + 1)^+$. HRMS, calculated for $C_{24}H_{30}N_6O_8P$ $(M + 1)^+$, 561.1863; found, 561.1871.

(2*S*)-(*S*)-*sec*-Butyl 2-((((2*R*,3*R*,4*R*,5*R*)-5-(4-Aminopyrrolo[1,2-*f*][1,2,4]triazin-7-yl)-5-cyano-3,4-dihydroxy-4-methyltetrahydrofuran-2-yl)methoxy)(phenoxy)phosphorylamino)propanoate (8). ^{1}H NMR (300 MHz, CD_3CN) δ 7.98 (s, 1H), 7.2−7.4 (m, 5H), 6.82 (d, 2H), 6.45 (s, 2H), 5.28 (d, 1H, OH), 4.81 (m, 1H, -OCH), 4.3−4.5 (m, 4H), 3.93 (m, 2H), 3.82 (t, 1H, 3′-CH), 1.56 (m, 2H), 1.35 (d, 3H), 1.17 (q, 3H, $CHCH_3$), 0.92 (s, 3H), 0.88 (m, 3H). ^{31}P NMR (121.4 MHz, CD_3CN) δ 3.19 (s). MS, *m/e* 589 $(M + 1)^+$.

(2*S*)-(*R*)-*sec*-Butyl 2-((((2*R*,3*R*,4*R*,5*R*)-5-(4-Aminopyrrolo[1,2-*f*][1,2,4]triazin-7-yl)-5-cyano-3,4-dihydroxy-4-methyltetrahydrofuran-2-yl)methoxy)(phenoxy)phosphorylamino)propanoate (9). ^{1}H NMR (300 MHz, DMSO-d_6) δ 7.89 (s, 1H), 7.85 (brs, 2H), 7.1−7.4 (m, 5H), 6.87 (2d, 1H), 6.78 (2d, 1H), 6.04 (m, 1H, NH), 5.97 (s, 1H), 5.42 (brt, 1H), 4.68 (m, 1H, -OCH), 4.1−4.5 (m, 3H), 3.82 (m, 1H), 3.65 (t, 1H, 3′-CH), 1.45 (m, 2H), 1.28 (d, 3H), 1.10 (d, 3H, $CHCH_3$), 0.89 (s, 3H), 0.77 (m, 3H). ^{31}P NMR (121.4 MHz, DMSO-d_6) δ 3.82, 4.01 (s). MS, *m/e* 589 $(M + 1)^+$. HRMS, calculated for $C_{26}H_{34}N_6O_8P$ $(M + 1)^+$, 589.2176; found, 589.2165.

(2*S*)-(*tert*-Butyl) 2-((((2*R*,3*R*,4*R*,5*R*)-5-(4-Aminopyrrolo[1,2-*f*][1,2,4]triazin-7-yl)-5-cyano-3,4-dihydroxy-4-methyltetrahydrofuran-2-yl)methoxy)(phenoxy)phosphorylamino)propanoate (10). ^{1}H NMR (300 MHz, $CDC1_3$) δ 8.02 (s, 1H), 7.1−7.3 (m, 5H), 6.80 (2d, 1H), 6.70 (2d, 1H), 6.01 (brs, 2H), 4.60 (m, 1H), 4.40 (m, 2H), 3.93 (m, 3H), 3.62 (s, 3H), 1.43 (2s, 9H), 1.37 (d, 3H), 0.90 (2s, 3H). ^{31}P NMR (121.4 MHz, $CDC1_3$) δ 2.89, 2.92 (s). MS, *m/e* 589 $(M + 1)^+$. HRMS, calculated for $C_{26}H_{34}N_6O_8P$ $(M + 1)^+$, 589.2176; found, 589.2180.

(2*S*)-*cyclo*-Pentyl 2-((((2*R*,3*R*,4*R*,5*R*)-5-(4-Aminopyrrolo[1,2-*f*][1,2,4]triazin-7-yl)-5-cyano-3,4-dihydroxy-4-methyltetrahydrofuran-2-yl)methoxy)(phenoxy)phosphorylamino)propanoate (11). ^{1}H NMR (300 MHz, $CDC1_3$) δ 7.97 (s, 1H), 7.1−7.3 (m, 5H), 6.72 (m, 2H), 6.40 (brs, 2H), 5.14 (m, 1H, OCH), 4.58 (m, 1H), 4.2−4.5 (m, 3H), 3.93 (m, 2H), 1.80 (m, 2H), 1.5−1.7 (m, 6H), 1.37 (d, 3H), 0.86 (s, 3H). ^{31}P NMR (121.4 MHz, $CDC1_3$) δ 2.89, 2.92 (s). MS, *m/e* 601 $(M + 1)^+$.

(2*S*)-*neo*-Pentyl 2-((((2*R*,3*R*,4*R*,5*R*)-5-(4-Aminopyrrolo[1,2-*f*][1,2,4]triazin-7-yl)-5-cyano-3,4-dihydroxy-4-methyltetrahydrofuran-2-yl)methoxy)(phenoxy)phosphorylamino)propanoate (12). ^{1}H NMR (300 MHz, CD_3CN) δ 7.98 (s, 1H), 7.2−7.4 (m, 5H), 6.82 (m, 2H), 6.44 (brs, 2H), 5.27 (s, 1H), 4.3−4.5 (m, 4H), 4.03 (m, 1H), 3.93 (m, 1H), 3.80 (m, 3H), 1.38 (d, 3H), 0.86 (m, 12H). ^{31}P NMR (121.4 MHz, CD_3CN) δ 3.14 (s). MS, *m/e* 603 $(M + 1)^+$. HRMS, calculated for $C_{27}H_{36}N_6O_8P$ $(M + 1)^+$, 603.2332; found, 603.2331.

(2*S*)-(2-Ethylbutyl) 2-((((2*R*,3*R*,4*R*,5*R*)-5-(4-Aminopyrrolo[1,2-*f*][1,2,4]triazin-7-yl)-5-cyano-3,4-dihydroxy-4-methyltetrahydrofuran-2-yl)methoxy)(phenoxy)phosphorylamino)propanoate (13). ^{1}H NMR (300 MHz, $CDC1_3$) δ 8.02 (s, 1H), 7.1−7.3 (m, 5H), 6.78 (2d, 1H), 6.65 (2d, 1H), 6.35 (brs, 1H), 6.02 (brs, 2H), 4.60 (m, 1H), 4.40 (m, 2H), 3.9−4.1 (m, 5H), 3.75 (brd, 1H), 1.50 (m, 1H), 1.3−1.4 (m, 7H), 0.86 (s, 9H). ^{31}P NMR (121.4 MHz, $CDC1_3$) δ 2.74, 2.75 (s). MS, *m/e* 617 $(M + 1)^+$. HRMS, calculated for $C_{28}H_{39}N_6O_8P$ $(M + 1)^+$, 617.2489; found, 617.2482.

(2*S*)-Benzyl 2-((((2*R*,3*R*,4*R*,5*R*)-5-(4-Aminopyrrolo[1,2-*f*][1,2,4]triazin-7-yl)-5-cyano-3,4-dihydroxy-4-methyltetrahydrofuran-2-yl)methoxy)(phenoxy)phosphorylamino)propanoate (14). ^{1}H NMR (300 MHz, DMSO-d_6) δ 7.91 (s, 1H), 7.85 (brs, 2H), 7.1−7.4 (m, 10H), 6.88 (2d, 1H), 6.77 (2d, 1H), 6.14 (m, 1H, NH), 5.95 (2s, 1H, 2′-OH), 5.41 (2d, 1H, 3′-OH), 5.02 (m, 2H, $PhCH_2$), 4.38 (m, 1H, 5′-CH_2), 4.21 (m, 1H, 5′-CH_2), 4.18 (m, 1H, 4′-CH), 3.92 (m, 1H, NHCH), 3.65 (t, 1H, 3′-CH), 1.22 (q, 3H, $CHCH_3$), 0.86 (s, 3H). ^{31}P NMR (121.4 MHz, DMSO-d_6) δ 3.84, 3.97 (s). MS, *m/e* 623 $(M + 1)^+$. HRMS, calculated for $C_{29}H_{32}N_6O_8P$ $(M + 1)^+$, 623.2019; found, 623.2017.

(2*S*)-Isopropyl 2-((((3a*R*,4*R*,6*R*,6a*R*)-6-(4-Aminopyrrolo[1,2-*f*][1,2,4]triazin-7-yl)-6-cyano-6a-methyl-2-oxotetrahydrofuro[3,4-*d*][1,3]dioxol-4-yl)methoxy)(phenoxy)phosphorylamino)propanoate (15). To a solution of compound **5** (100 mg, 0.174 mmol) in acetonitrile (10 mL) was added carbodiimidazole (60 mg, 0.370 mmol), and the reaction mixture was stirred at room temperature for 6 h. Water (0.2 mL) was added, and the reaction mixture was stirred for 0.5 h. The mixture was concentrated and partitioned between ethyl acetate and water. The organic layer was concentrated, and the residue was purified by silica gel column chromatography (ethyl acetate−5% ethanol in ethyl acetate), affording the product **15** (90 mg, 86%) as a solid. ^{1}H NMR (300 MHz, $CDC1_3$) δ 8.08 (s, 1H), 7.1−7.4 (m, 5H), 6.9 (2d, 1H), 6.7 (2d, 1H), 5.84 (brs, 2H), 5.01 (m, 1H), 4.8 (2d, 1H), 4.4−4.6 (m, 2H), 3.9−4.1 (m, 3H), 1.41 (d, 3H), 1.3 (m, 6H), 1.1 (2s, 3H). ^{31}P NMR (121.4 MHz, $CDC1_3$) δ 2.74, 2.88 (s). MS, *m/e* 601 $(M + 1)^+$.

(2*S*)-Isopropyl 2-((((2*R*,3*R*,4*R*,5*R*)-3-Isobutyroxy-5-(4-aminopyrrolo[1,2-*f*][1,2,4]triazin-7-yl)-5-cyano-4-hydroxy-4-methyltetrahydrofuran-2-yl)methoxy)(phenoxy)-phosphorylamino)propanoate (16). To a solution of compound **5** (175 mg, 0.305 mmol) in acetonitrile (2 mL) was added *N*,*N*-dimethyformamide dimethyl acetal (41 μL, 0.34 mmol, 1.1 equiv), and the reaction mixture was stirred at room temperature for 1 h. The reaction was complete (by LCMS). The mixture was then concentrated to dryness. To the residue was added DCC (250 mg, 1.21 mmol, 4 equiv), acetonitrile (5 mL), and isobutyric acid (55 mg, 58 μL, 2 equiv). The mixture was stirred at room temperature for 48 h. Water (0.2 mL) and trifluoroacetic acid (0.1 mL) were added at 0 °C, and the reaction mixture was stirred at room temperature for 64 h. Sodium bicarbonate (500 mg) was added at 0 °C. The mixture was stirred at room temperature for 0.5 h and filtered. The filtrate was concentrated, and the residue was purified by silica gel column chromatography (5% methanol/dichloromethane), affording compound **16** as a 1:1 diastereomeric mixture at phosphorus (144 mg, 73%). ^{1}H NMR (300 MHz, $CDC1_3$) δ 8.00 (s, 1H), 7.1−7.4 (m, 5H), 6.83 (d, 1H), 6.71 (2d, 1H), 5.97 (brs, 2H), 5.94 (d, 1H), 5.07 (2d, 1H), 5.01 (m, 1H), 4.68 (m, 1H), 4.4 (m, 2H), 4.0 (m, 2H), 2.74 (m, 1H), 1.4 (2d, 3H), 1.2−1.3 (12H), 0.98 and 0.99 (2s, 3H). ^{31}P NMR

dx.doi.org/10.1021/jm400201a | *J. Med. Chem.* XXXX, XXX, XXX−XXX

(121.4 MHz, $CDCl_3$) δ 2.56, 2.65 (s). MS, *m/e* 645 $(M + 1)^+$. HRMS, calculated for $C_{29}H_{38}N_6O_9P$ $(M + 1)^+$, 645.2432; found, 645.2434.

(2*S*)-Isopropyl 2-((4-Nitrophenoxy)(phenoxy)-phosphorylamino)propanoate (28). To a suspension of L-alanine isopropyl ester hydrochloride (7.95 g, 47.4 mmol) in dichloromethane (100 mL) was added phenyl phosphorodichloridate (10 g, 47.4 mmol). After cooling to −20 °C, triethylamine (13.2 mL, 95 mmol) was dropwise added over a period of 15 min (internal reaction temperature; −10 °C ∼ −3 °C). When the reaction was almost complete (by phosphorus NMR), *p*-nitrophenol (6.29 g, 45.0 mmol) was added as a solid in one portion. Additional triethylamine (6.28 mL, 45 mmol) was added over a period of 15 min. The mixture was then warmed up to room temperature. When the reaction was complete, MTBE (100 mL) was added. The white precipitate was removed by filtration. The filter cake was washed with MTBE (3 × 50 mL). The filtrate and the washings were combined and concentrated. The residue was purified by silica gel column chromatography (0−50% ethyl acetate/hexanes), affording compound **28** as a 1:1 ratio of a diasteromeric mixture (14.1 g, 77%). ^{1}H NMR (300 MHz, $CDCl_3$): δ 8.22 (2d, 2H), 7.2−7.4 (m, 7H), 5.0 (m, 1H), 4.09 (m, 1H), 3.96 (m, 1H), 1.39 (2d, 3H), 1.22 (m, 6H). MS, *m/e* 409 $(M + 1)^+$.

Separation of the Two Diastereomers of 28. The two diastereomers were separated by chiral column chromatography under the following conditions: column, Chiralpak IC, 2 cm × 25 cm; solvent system, 70% heptane and 30% isopropanol (IPA); flow rate, 6 mL/min; loading volume per run, 1.0 mL; concentration of loading sample, 150 mg/mL in 70% hepane and 30% IPA. (*Sp*)-**28**: retention time 43 min. ^{31}P NMR (161.9 MHz, $CDCl_3$): δ −2.99 (s). (*Rp*)-**28**: retention time 62 min. ^{31}P NMR (161.9 MHz, $CDCl_3$): δ −3.02 (s).

Alternatively, the two diasteromers were separated by crystallization under the following procedures:

Diastereomeric mixture **28** was dissolved in diethyl ether (∼10 mL/g). While stirring, hexanes was then added until the solution became turbid. Seed crystals (∼10 mg/g of compound **C**) were added to promote crystallization. The resulting suspension was gently stirred for 16 h, cooled to ∼0 °C, stirred for an additional 2 h, and filtered to collect the crystalline material (recovery yield of the crystalline material ∼35%). The crystalline material contains ∼95% of (*Sp*)-**28** and ∼5% of (*Rp*)-**28**. Recrystallization afforded >99% diastereomerically pure (*Sp*)-**28**.

(*Sp*)-Isopropyl 2-((*S*)-(((2*R*,3*R*,4*R*,5*R*)-5-(4-aminopyrrolo[1,2-*f*][1,2,4]triazin-7-yl)-5-cyano-3,4-dihydroxy-4-methyltetrahydrofuran-2-yl)methoxy)(phenoxy)phosphorylamino)-propanoate (17). To a dry, argon purged round-bottom flask were added compound **2** (1.0 g, 3.28 mmol) and anhydrous THF (15 mL). The slurry was stirred for 10 min, and the flask was place in a water bath at room temperature. *t*-Butylmagnesium chloride in THF (1.0 M, 4.91 mL) was dropwise added, and the mixture was stirred for an additional 10 min. A solution of (*Sp*)-**28** (2.68 g, 6.55 mmol) in THF (10 mL) was then added. The flask was place in a heating oil bath preset at 50 °C, and the mixture was stirred until compound **2** was almost consumed. After ∼2.5 h, the reaction mixture was cooled to room temperature, and methanol (5 mL) was added. Solvents were removed under reduced pressure, and the residue was purified by silica gel column chromatography (70% ethyl acetare/hexanes to remove less polar impurities, 10% methanol/dichloromethane to elute the product), affording **17** as an off-white solid (1.45 g, 77%). ^{1}H NMR (400 MHz, DMSO-d_6): δ 7.89 (s, 1H), 7.84 (brs, 2H), 7.36 (t, 2H), 7.23 (d, 2H), 7.17 (t, 1H), 6.87 (d, J = 4.4 Hz, 1H), 6.74 (d, J = 4.4 Hz, 1H), 6.02 (dd, 1H), 5.96 (s, 1H), 5.41 (d, 1H), 4.82 (m, 1H), 4.38 (dd, 1H), 4.22 (q, 1H), 4.16 (m, 1H), 3.81 (m, 1H), 3.67 (dd, 1H), 1.22 (d, 3H), 1.11 (dd, 6H), 0.89 (s, 3H). ^{31}P NMR (161.9 MHz, DMSO-d_6): δ 3.99 (s). MS, *m/e* 575 $(M + 1)^+$, 573 $(M - 1)^-$. HRMS, calculated for $C_{25}H_{32}N_6O_8P$ $(M + 1)^+$, 575.2014; found, 575.2022.

(*Sp*)-Isopropyl 2-((*S*)-(((2*R*,3*R*,4*R*,5*R*)-3-isobutyroxy-5-(4-aminopyrrolo[1,2-*f*][1,2,4]triazin-7-yl)-5-cyano-4-hydroxy-4-methyltetrahydrofuran-2-yl)methoxy)(phenoxy)-phosphorylamino)propanoate (18). Compound **18** was prepared by following the procedure for **16** except using **17** as the starting material instead of **5**. ^{1}H NMR (300 MHz, $CDCl_3$) δ 8.00 (s, IH), 7.1−7.3 (m, 5H), 6.83 (d, IH), 6.71 (d, IH), 6.09 (brs, 2H), 5.95 (s, IH), 5.04 (m, 2H), 4.67 (q, IH), 4.35−4.52 (m, 2H), 4.00 (m, 2H), 2.74 (m, IH), 1.40 (d, 3H), 1.2−1.3 (12H), 0.98 (s, 3H). ^{31}P NMR (121.4 MHz, $CDCl_3$) δ 2.72 (s). HRMS, calculated for $C_{29}H_{38}N_6O_9P$ $(M + 1)^+$, 645.2432; found, 645.2434. The compound was subsequently recrystallized from MTBE for X-ray quality crystals.

HCV Replicon Antiviral and Cytotoxicity Assays. All compounds were supplied in 100% DMSO. Compound serial dilutions were performed in 100% DMSO. For EC_{50} and CC_{50} determinations, test compounds were serially diluted in ten steps of 1:3 dilutions in 384-well plates. All serial dilutions were performed in four replicates per compound within the same 384-well plate. An HCV protease inhibitor ITMN-191 at 100 μM was added as a control of 100% inhibition of HCV replication while puromycin at 10 mM was included as a control of 100% cytotoxicity. To each well of a black polystyrene 384-well plate (Greiner Bio-one, Monroe, NC), 90 μL of cell culture medium (without Geneticin) containing 2000 suspended HCV replicon cells was added with a Biotek μFlow workstation. For compound transfer into cell culture plates, 0.4 μL of compound solution from the compound serial dilution plate was transferred to the cell culture plate on a Biomek FX workstation. The DMSO concentration in the final assay wells was 0.44%. The plates were incubated for 3 days at 37 °C with 5% CO_2 and 85% humidity. The HCV replicon assay was a multiplex assay, able to assess both cytotoxicity and antireplicon activity from the same well. The CC_{50} assay was performed first. The media in the 384-well cell culture plate was aspirated, and the wells were washed four times with 100 μL of PBS each, using a Biotek ELX405 plate washer. A volume of 50 μL of a solution containing 400 nM calcein AM (Anaspec, Fremont, CA) in 1 × PBS was added to each well of the plate with a Biotek μFlow workstation. The plate was incubated for 30 min at room temperature before the fluorescence signal (excitation 490 nm, emission 520 nm) was measured with a Perkin-Elmer Envision plate reader.

The EC_{50} assay was performed in the same wells as the CC_{50} assay. The calcein-PBS solution in the 384-well cell culture plate was aspirated with a Biotek ELX405 plate washer. A volume of 20 μL of Dual-Glo luciferase buffer (Promega, Madison, WI) was added to each well of the plate with a Biotek μFlow Workstation. The plate was incubated for 10 min at room temperature. A volume of 20 μL of a solution containing a 1:100 mixture of Dual-Glo Stop & Glo substrate (Promega, Madison, WI) and Dual-Glo Stop & Glo buffer (Promega, Madison, WI) was added to each well of the plate with a Biotek μFlow Workstation. The plate was then incubated at room temperature for 10 min before the luminescence signal was measured with a Perkin-Elmer Envision Plate Reader.

Data Analysis. The cytotoxicity effect was determined by calcein AM conversion to fluorescent product. The percent cytotoxicity was calculated by eq 1:

$$\%\text{cytotoxicity or }\%\text{inhibition} = 100 \times \left(1 - \frac{X_C - M_B}{M_D - M_B}\right) \quad (1)$$

where X_C is the fluorescence signal from compound treated well; M_B is the average fluorescence signal from puromycin treated wells; and M_D is the average fluorescence signal from DMSO treated wells. The percent anti-HCV replication activity was determined by the luminescence signal generated from the renilla luciferase reporter of the HCV replicon. The percent inhibition of HCV replicon was calculated using eq 1, where X_C is the luminescence signal from the compound treated well; M_B is the average luminescence signal from ITMN-191 treated wells; and M_D is the average luminescence signal from DMSO treated wells.

The CC_{50} values were determined as the testing compound concentration that caused a 50% decrease of cell viability. The EC_{50} values were determined as the testing compound concentration that caused a 50% decrease in HCV replication. Both CC_{50} and EC_{50} values were obtained using the Pipeline Pilot 5.0 software package (Accelrys, San Diego, CA) by nonlinear regression fitting of experimental data to eq 2:

dx.doi.org/10.1021/jm400201a | J. Med. Chem. XXXX, XXX, XXX−XXX

$$y = d + \frac{a - d}{\left[1 + \left(\frac{x}{c}\right)^{b}\right]} \quad (2)$$

where y is the observed %inhibition of the HCV replicon at x concentration of compound; d is the estimated response at zero compound concentration; a is the estimated response at infinite compound concentration; c is the midrange concentration (CC_{50} or EC_{50}); and b is the Hill slope factor.

HCV Polymerase (NS5B) Enzyme Assay. Inhibition of NS5B was studied using GT1b NS5B recombinant protein. All concentrations are final concentrations. In a solution containing 50 mM Tris-HCl (pH 7.5), 10 mM KCl, 1 mM DTT, 5 mM $MgCl_2$, 0.2 unit/μL RNAsin (Promega), and 0.01% BSA, 75 nM NS5B was preincubated with 4 ng/μL (50 nM) heteropolymer RNA template (sshRNA) (reference: Hung M.; Gibbs, C. S.; Tsiang, M. Biochemical characterization of rhinovirus RNA-dependent RNA polymerase. *Antiviral Res.* **2002**, *56* (2), 99−114) at RT for 5 min, followed by the addition and incubation of the inhibitors at RT for 5 min. The reaction was started by addition of a mixture of ATP (2.5 μM), CTP (2.5 μM), UTP (2.5 μM), 0.03 μM ^{33}P-labeled GTP (Perkin-Elmer, NEG603H, 3000 Ci/mmol, 3.3 μM), and 1.25 μM GTP. After 90 min of incubation at 30 °C, the reaction mixture was spotted on DE-81 filter paper and washed with 0.125 mM Na_2HPO_4 (3×), distilled water (1×), and reagent ethanol (1×). The filter paper was air-dried and exposed to phosphoimager (Typhooh, GE), and the data was analyzed using ImageQuant software (GE).

Single Nucleotide Incorporation by Mitochondrial RNA Polymerase (POLRMT). A mixture of MTCN buffer (50 mM MES, 25 mM Tris-HCl, 25 mM CAPS, and 50 mM NaCl, pH 7.5), 200 nM 5′-^{32}P-R12/D18 (reference Arnold 2012 PLoSPathogen), 10 mM $MgCl_2$, 1 mM DTT, and 376 nM POLRMT (Enzymax, Lexington, KY) was preincubated at 30 °C for 1 min. The reaction was started by addition of 500 μM (final) natural NTP or NTP analogs. At selected time points, the reaction mixture was removed and quenched with gel loading buffer containing 100 mM EDTA, 80% formamide, and bromophenol blue, and heated at 65 °C for 5 min. The samples were run on a 20% polyacrylamide gel (8 M urea), and the product formation was quantified using Typhoon Trio Imager and Image Quant TL Software (GE Healthcare, Piscataway, NJ). The rate of single nucleotide incorporation by mt RNA pol was calculated by fitting the product formation using the single exponential equation: $[R13] = A(1 - e^{-kt})$, where [R13] represents the amount (in nM) of the elongated product formed, t represents the reaction time, k represents the observed rate, and A represents the amplitude of the exponential.

Measurements of Triphosphate Levels in Replicon Cells. Replicon cells (Huh-7 cells) were maintained in Dulbecco's modified eagle medium containing glutamax supplemented with 10% heat inactivated fetal bovine serum, penicillin-streptomycin, and G418 disulphate salt solution. Cells were transferred to 12-well tissue culture treated plates by trypsonization and grown to confluency (0.88×10^6 cells/well). Cells were treated for 24 h with a test compound (10 μM). Following 24 h, cells were washed twice with 2.0 mL of ice cold 0.9% sodium chloride saline. Cells were then scraped into 0.5 mL of 70% methanol and frozen overnight to facilitate the extraction of nucleotide metabolites. Extracted cell material in 70% methanol was transferred into tubes and dried. After drying, samples were resuspended in 1 mM ammonium phosphate pH 8.5. TP levels were quantified using liquid chromatography coupled to triple quadrapole mass spectrometry by methods similar to those previously reported in Durand-Gasselin, L.; Van Rompay, K. K.; Vela, J. E.; Henne, I. N.; Lee, W. A.; Rhodes, G. R. *Mol. Pharm.* **2009**, *6*, 1145.

Measurement of Triphosphate Levels in Primary Human Hepatocytes. Primary human hepatocytes were maintained in Williams E medium containing Cellz Direct's proprietary supplement cocktail. Cells were purchased from Cellz Direct as a twelve well plate format grown to confluency (0.88×10^6 cells/well). Cells were treated for 1 h with a test compound (10 μM) followed by a 23 h treatment with nondrug containing media. Cells were collected at 0, 0.5, and 1 h during compound incubation and at 0, 0.5, 1, 3, 6, 8, and 23 h following compound removal. Cells were collected, and intracellular metabolites were analyzed as described for replicon cells.

Caco-2 Permeability. Bidirectional permeability studies were done using confluent conolayers of the human colon carcinoma cell line (caco-2). Caco-2 cells were grown to confluence over at least 21 days on 24 well PET (polyethylene-terephthalate) plates (BD Biosciences). After an initial equilibration with transport buffer, TEER values were read to test membrane integrity. The experiment was started by the addition of buffers containing test compound, and the samples were taken at 1 and 2 h from the receiver compartment. All samples were immediately precipitated by 4 volumes of 100% acetonitrile containing internal standard and analyzed by LC/MS/MS. The compound was tested in 2 separate replicate wells for each condition, and the permeability of control compounds (atenolol, propranolol, and vinblastine) was determined to meet acceptance criteria for each batch of assay plates. Cells were dosed on the apical (A) or basolateral (B) side to determine forward (A to B) and reverse (B to A) permeability. Permeability through a cell free trans-well was also determined as a measure of cellular permeability through the membrane. To test for nonspecific binding and compound instability, the total amount of drug was quantified at the end of the experiment and compared to the material present in the original dosing solution as a percent recovery.

The apparent permeability, P_{app}, and % recovery were calculated as follows:

$$P_{app} = (dR/dt)V_r/(AD_0)$$

$$\%\text{Recovery} = 100((V_rR_{120}) + (V_dD_{120}))/(V_dD_0)$$

where dR/dt is the slope of the cumulative concentration in the receiver compartment versus time in μM/s based on receiver concentrations measured at 60 and 120 min, V_r and V_d are the volume in the receiver and donor compartments in cm^3, respectively, A is the area of the cell monolayer (0.33 cm^2), D_0 and D_{120} are the measured donor concentrations at the beginning and end of the experiment, respectively, and R_{120} is the receiver concentration at the end of the experiment (120 min).

Intestinal and Hepatic S9 Stability. The compounds were incubated at 2 μM in human intestinal and hepatic S9 fractions (obtained from In Vitro Technologies, Baltimore, MD) for 90 min at 37 °C in the presence of NADPH and UDPGA (phase I and phase II cofactor, Sigma-Aldrich). At specified time points following compound addition, samples were quenched with nine volumes of an aqueous solution containing internal standard, 50% acetonitrile, and 25% methanol. Sample plates were centrifuged at 3000g for 30 min, and 10 μL of the resulting solution was analyzed by LC/MS/MS. Data (sample to internal standard peak area ratio) were plotted on a semi log scale and fitted using an exponential fit. Assuming first-order kinetics, the half-life and rate of metabolism were determined. Predicted hepatic extraction was calculated from the half-life by reported methods using the well-stirred model for hepatic clearance.

LC/MS/MS Instrumentation. S9 stability and caco-2 assay: Liquid chromatography was performed using an Agilent 1200-series quaternary pump system (Agilent Technologies, Santa Clara, CA) with a 2 μm 20 × 2.1 mm Mercury RP C_{18} (Phenomenex, Torrance, CA) for S9 stability assay samples, and a 1.7 μm 50 × 2.1 mm Acquity UPLC BEH C_{18} (Waters, Milford, MA) for caco-2 assay samples. A HPLC system was coupled to a Quattro Premier triple-quadrupole mass spectrometer (Waters, Milford, MA). Mass spectrometry was performed in positive-ion mode and multiple reaction monitoring modes using a Quattro Premier (Waters, Milford, MA). The test compound was eluted with a mobile phase consisting of 0.2% formic acid and a linear gradient from 0 to 95% acetonitrile over 2 min.

log *D* Measurement. A solution of test compound in DMSO (2 μL of 10 mM) was added into a 96-well plate containing 198 μL of 1:1 acetonitrile/water. The sample plate was shaken for 30 min, and 10 μL of the resulting solution was analyzed by HPLC/UV. The instrumentation used was an Alliance 2795 HPLC coupled with a photodiode array detector 2996 (Waters, Milford, MA) using a Waters

dx.doi.org/10.1021/jm400201a | J. Med. Chem. XXXX, XXX, XXX−XXX

XTerra 3.5 μm 4.6 mm × 50 mm C_{18} column. The mobile phase consisted of solvent A (20 mM ammonium acetate aqueous solution) and solvent B (100% acetonitrile). Elution was performed using a linear gradient of solvent B from 0% to 100% in 8 min. The log *D* value was calculated using the retention time of test compound compared to the reference compounds. The range of log *D* values for reference compounds is approximately between 0.3 and 5.7.

Aqueous Solubility. The aqueous solubility of the test compounds was determined at ambient temperature using pH 2 hydrochloric acid and pH 7 phosphate buffer. Excess solid drug substance was used to saturate the solution media. The resultant suspensions were sonicated using a sonication bath (VWR model 250T, VWR International LLC, Radnor, PA, or Branson model 2510, Branson Ultrasonic Corporation, Danbury, CT) and were then stirred for at least 2 h at ambient temperature using a stir plate (IKAMAG, IKA Works, Inc., Wilmington, NC) or a Thermomixer (Eppendorf AG, Hamburg, Germany). The samples were subsequently centrifuged (Eppendorf Centrifuge, Eppendorf AG, Hamburg, Germany), and the supernatant was assayed for test compound using a standard reverse-phase UPLC-UV method with an ACE C18, 50 mm × 2.1 mm, 3 μm particle column (Advanced Chromatography Technologies, Aberdeen, U.K.).

Hamster Liver Triphosphate Analysis. Groups of 12 Golden Syrian hamsters were administered a test compound intravenously at 1 mg-equiv/kg and orally at 5 mg-equiv/kg. Formulation consisted of EtOH, PEG400, and water and was adjusted to pH 4 by HCl (0.5 mg-equiv/mL) for iv dosing and buffered with 50 mM pH 4 citrate (2.5 mg-equiv/mL) for oral dosing. At 1, 4, 8, and 12 h, livers were harvested under isoflurane anesthesia. Collected livers were wrapped in aluminum foil and snap-frozen in liquid nitrogen immediately following removal to avoid sample dephosphorylation. Livers were processed by sectioning into smaller pieces with a razor blade and collecting into preweighed 15 mL conical tubes kept on dry ice. Four volumes of ice-cold extraction buffer (0.1% KOH and 67 mM EDTA in 70% MeOH, containing 0.25 μM Cl-ATP) were added, and samples were promptly homogenized using an Omni-Tip TH with disposable, hard tissue homogenizer probes (Omni International). Aliquots of homogenate were then centrifuged (20,000*g* at 4 °C for 10 min). Aliquots of supernatant were transferred to clean tubes, evaporated to dryness in a heated centrifugal evaporator, and reconstituted with an equal volume of 1 mM ammonium phosphate (pH 7.0). Intracellular triphosphate levels were measured by LC/MS/MS as described for samples generated in vitro. Levels of endogenous adenosine triphosphate were also determined to ensure the sample stability.

Dog in Vivo Pharmacokinetic Analysis. Groups of three non-naïve male beagle dogs were administered a single dose of a test compound by intravenous infusion at 0.5 mg/kg or orally at 5 mg/kg. The intravenous dosing was done in 5/20/75 (EtOH/PEG 400/water, pH 4 w/HCl), and the oral formulation was made up in 5/40/55 (EtOH/PEG 400/50 mM citrate buffer, pH 4). Blood samples were collected over a 24 h period postdose into Vacutainer tubes containing EDTA-K3 (BD Biosciences), and plasma was isolated by the manufacturer's suggested protocol. Plasma samples were processed via protein precipitation by adding acetonitrile to a final concentration of 60%. Following filtration to remove precipitated proteins, samples were dried and reconstituted in 20% acetonitrile in water. Samples were then analyzed by reversed phase liquid chromatography coupled to a triple quadrapole mass spectrometer (LC/MS/MS) in positive ion and multiple reaction monitoring modes. Percent oral absorption (% F_a) was determined as follows:

% oral absorption

$$\%F_a = \%F/(1 - E_H)$$

hepatic extraction

$$E_H = (AUC_{portal} - AUC_{systemic})/AUC_{portal}$$

oral bioavailability

$$\%F = AUC_{po} \times Dose_{iv}/AUC_{iv} \times Dose_{po}$$

Liver triphosphate levels were determined by a method similar to that described in hamster PK analysis.

■ ASSOCIATED CONTENT

Ⓢ Supporting Information

Tables for pan-genotypic activity of **18** (Table S1), resistant profile of **16** (Table S2), and in vitro activity of **16** in combination with other classes of anti-HCV agents (Table S3). This material is available free of charge via the Internet at http://pubs.acs.org.

Accession Codes

The Cambridge Crystallographic Data Center (CCDC) numbers for X-ray structures of compounds (*Sp*)-**28** and **18** are 929320 and 929321, respectively.

■ AUTHOR INFORMATION

Corresponding Author

*Phone: 650-522-5177. Fax: 650-5225899. E-mail: Aesop.Cho@gilead.com.

Notes

The authors declare the following competing financial interest(s): The authors are employees of Gilead Sciences (except W. Zhong, S. Rossi, M. Fenaux, and C. Kim, who were employed at Gilead Sciences during this work). All authors are shareholders in Gilead Sciences.

■ ACKNOWLEDGMENTS

We thank Amy Kowk for assisting with chiral column separation, Tim S. Lane for obtaining HRMS, and Arnold Rheingold (UCSD) for X-ray crystal structures.

■ ABBREVIATIONS USED

HCV, hepatitis C virus; NI, nucleoside inhibitor; NS5B, nonstructural protein 5B; SOC, standard of care; Peg-IFN, pegylated interferon-α; RBV, ribavirin; DAA, direct-acting antiviral; NOAEL, no-observable adverse effects level; POLRMT, mitochondrial RNA polymerase; SVR, sustained virologic response; DMPK, drug metabolism and pharmacokinetics; GT, genotype; NS5A, nonstructural protein 5A; NS3, nonstructural protein 3; BID, twice daily; PK/PD, pharmacokinetic/pharmacodynamic; MTCN, MES-TRIS-CAPS-NaCl; MES, 2-(*N*-morpholino)ethanesulfonic acid; TRIS, tris-(hydroxymethyl)aminomethane; CAPS, *N*-cyclohexyl-3-amino-propanesulfonic acid; NTP, nucleoside triphosphate; NADPH, nicotinamide adenine dinucleotide phosphate; UDPGA, uridine 5′-diphospho-glucuronic acid; Cl-ATP, 2-choloroadenosine triphosphate

■ REFERENCES

(1) Lavanchy, D. Evolving epidemiology of hepatitis C virus. *Clin. Microbiol. Infect.* **2011**, *17*, 107−115.

(2) Zeuzem, S.; Berg, T.; Moeller, B.; Hinrichsen, H.; Mauss, S.; Wedemeyer, H.; Sarrazin, C.; Hueppe, D.; Zehnter, E.; Manns, M. P. Expert opinion on the treatment of patients with chronic hepatitis C. *J. Viral Hepatitis* **2009**, *16*, 75−90.

(3) (a) Vachon, M.-L.; Dieterich, D. T. The era of direct-acting antivirals has begun: The beginning of the end for HCV. *Semin. Liver Dis.* **2011**, *31*, 399−409. (b) Kronenberger, B.; Zeuzem, S. New developments in HCV therapy. *J. Viral Hepatitis* **2012**, *19*, 48−51.

(4) Manns, M. P.; Foster, G. R.; Rockstroh, J. K.; Zeuzem, S.; Zoulim, F.; Houghton, M. The way forward in HCV treatment - finding the right path. *Nat. Rev. Drug Discovery* **2007**, *6*, 991−1000.
(5) Stedman, C. A. M. Current prospects for interferon-free treatment of hepatitis C in 2012. *J. Gastroenterol. Hepatology* **2013**, *28* (1), 38−45.
(6) Sofia, M. J. Nucleotide prodrugs for HCV therapy. *Antiviral Chem. Chemother.* **2011**, *22*, 23−49.
(7) (a) Mericitabine (R7128): Ali, S.; Leveque, V.; Pogam, S. L.; Ma, H.; Philipp, F.; Inocencio, N.; Smith, M.; Alker, A.; Kang, H.; Najera, I.; Klumpp, K.; Symons, J.; Cammack, N.; Jiang, W.-R. Selected Replicon Variants with Low-Level In Vitro Resistance to the Hepatitis C Virus NS5B Polymerase Inhibitor PSI-6130 Lack Cross-Resistance with R1479. *Antimicrob. Agents Chemother.* **2008**, *52*, 4356−4369. (b) BMS-986094 (INX-08189): McGuigan, C.; Madela, K.; Aljarah, M.; Gilles, A.; Brancale, A.; Zonta, N.; Chamberlain, S.; Vernachio, J.; Hutchins, J.; Hall, A.; Ames, B.; Gorovits, E.; Ganguly, B.; Kolykhalov, A.; Wang, J.; Muhammad, J.; Patti, J. M.; Henson, G. Design, synthesis and evaluation of a novel double pro-drug: INX-08189. A new clinical candidate for hepatitis C virus. *Bioorg. Med. Chem. Lett.* **2010**, *20*, 4850−4854. (c) IDX-184: Zhou, X.-J.; Pietropaolo, K.; Chen, J.; Khan, S.; Sullivan-Bolyai, J.; Mayers, D. Safety and Pharmacokinetics of IDX184, a Liver-Targeted Nucleotide Polymerase Inhibitor of Hepatitis C Virus in Healthy Subjects. *Antimicrob. Agents Chemother.* **2011**, *55*, 76−81.
(8) GS-7977 (PSI-7977): Sofia, M. J.; Bao, D.; Chang, W.; Du, J.; Nagarathnam, D.; Rachakonda, S.; Reddy, P. G.; Ross, B. S.; Wang, P.; Zhang, H.-R.; Bansal, S.; Espiritu, C.; Keilman, M.; Lam, A. M.; Steuer, M.; Niu, C.; Otto, M. J.; Furman, P. S. Discovery of a β-D-2′-Deoxy-2′-α-fluoro-2′-β-*C*-methyluridine Nucleotide Prodrug (PSI-7977) for the Treatment of Hepatitis C Virus. *J. Med. Chem.* **2010**, *53*, 7202−7218.
(9) (a) Jenkins, S. R.; Arison, B.; Walton, E. Branched-chain sugar nucleosides. *J. Org. Chem.* **1968**, *33*, 2490−2494. (b) Walton, E.; Jenkins, S. R.; Nutt, R. F.; Holly, F. W. Branched-chain sugar nucleosides. V. Synthesis and antiviral properties of several branched-chain sugar nucleosides. *J. Med. Chem.* **1969**, *12*, 306−309.
(10) Carroll, S. S.; Tomassini, J. E.; Bosserman, M.; Getty, K.; Stahlhut, M. W.; Eldrup, A. B.; Bhat, B.; Hall, D.; Simcoe, A. L.; LaFemina, R.; Rutkowski, C. A.; Wolanski, B.; Yang, Z.; Migliaccio, G.; Francesco, R. D.; Kuo, L. C.; MacCoss, M.; Olsen, D. B. Inhibition of Hepatitis C Virus RNA Replication by 2′-Modified Nucleoside Analogs. *J. Biol. Chem.* **2003**, *278*, 11979−11984.
(11) Migliaccio, G.; Tomassini, J. E.; Carroll, S. S.; Tomei, L.; Altamura, S.; Bhat, B.; Bartholomew, L.; Bosserman, M. R.; Ceccacci, A.; Colwell, L. F.; Cortese, R.; Francesco, R. D.; Eldrup, A. B.; Getty, K. L.; Hou, Z. S.; LaFemina, R. L.; Ludmerer, S. W.; MacCoss, M.; McMasters, D. R.; Stahlhut, M. W.; Olsen, D. B.; Hazuda, D. J.; Flores, O. A. Characterization of Resistance to Non-obligate Chain-terminating Ribonucleoside Analogs That Inhibit Hepatitis C Virus Replication *in Vitro*. *J. Biol. Chem.* **2003**, *278*, 49164−49170.
(12) Cho, A.; Zhang, L.; Xu, J.; Babusis, D.; Butler, T.; Lee, R.; Saunders, O. L.; Wang, T.; Parrish, J.; Perry, J.; Feng, J. Y.; Ray, A. S.; Kim, C. U. Synthesis and characterization of 2'-*C*-Me branched *C*-nucleosides as HCV polymerase inhibitors. *Bioorg. Med. Chem. Lett.* **2012**, *22*, 4127−4132.
(13) Olsen, D. B.; Eldrup, A. B.; Bartholomew, L.; Bhat, B.; Bosserman, M. R.; Ceccacci, A.; Colwell, L. F.; Fay, J. F.; Flores, O. A.; Getty, K. L.; Grobler, J. A.; LaFemina, R. L.; Markel, E. J.; Migliaccio, G.; Prhavc, M.; Stahlhut, M. W.; Tomassini, J. E.; MacCoss, M.; Hazuda, D. J.; Carroll, S. S. A 7-Deaza-Adenosine Analog Is a Potent and Selective Inhibitor of Hepatitis C Virus Replication with Excellent Pharmacokinetic Properties. *Antimicrob. Agents Chemother.* **2004**, *48*, 3944−3953.
(14) Carroll, S. S.; Ludmerer, S.; Handt, L.; Koeplinger, K.; Zhang, N. R.; Graham, D.; Davies, M.-E.; MacCoss, M.; Hazuda, D.; Olsen, D. B. Robust Antiviral Efficacy upon Administration of a Nucleoside Analog to Hepatitis C Virus-Infected Chimpanzees. *Antimicrob. Agents Chemother.* **2009**, *53*, 926.
(15) Cho, A.; Saunders, O. L.; Butler, T.; Zhang, L.; Xu, J.; Vela, J. E.; Feng, J. Y.; Ray, A. S.; Kim, C. U. Synthesis and antiviral activity of a series of 1′-substituted 4-aza-7,9-dideazaadenosine *C*-nucleosides. *Bioorg. Med. Chem. Lett.* **2012**, *22*, 2705−2707.
(16) Lawitz, E.; Hill, J.; Marbury, T.; Hazan, L.; Gruener, D.; Webster, L.; Majuskas, R.; Morrison, R.; DiMicco, M.; German, P.; Stefanidis, D., Svaroskaia, E.; Jain, A.; Arterburn, S.; Ray, A.; Rossi, S.; McHutchison, J.; Rodriguez-Torres, M. GS-6620, A Liver-Targeted Nucleotide Prodrug, Exhibits Antiviral Activity and Favorable Safety Profile over 5 days in Treatment Naïve Chronic HCV Genotype 1 Subjects. *EASL*, 2012; poster 1188.
(17) Bushnell, D. A.; Cramer, P.; Kornberg, R. D. Structural basis of transcription: α-Amanitin−RNA polymerase II cocrystal at 2.8 Å resolution. *Proc. Natl. Acad. Sci. U.S.A.* **2002**, *99*, 1218−1222.
(18) Arnold, J. J.; Sharma, S. D.; Feng, J. Y.; Ray, A. S.; Smidansky, E. D.; Kireeva, M. L.; Cho, A.; Perry, J.; Vela, J. E.; Park, Y.; Xu, Y.; Tian, Y.; Babusis, D.; Barauskus, O.; Peterson, B. R.; Gnatt, A.; Kashlev, M.; Zhong, W.; Cameron, C. E. Sensitivity of mitochondrial transcription and resistance of RNA polymerase II dependent nuclear transcription to antiviral ribonucleosides. *PLoS Pathog.* **2012**, *8* (11), e1003030.
(19) Ray, A. S; Karl Y. Hostetler, K. Y. Application of kinase bypass strategies to nucleoside antivirals. *Antiviral Res.* **2011**, *92*, 277−291.
(20) Gane, E. J.; Stedman, C. A.; Hyland, R. H.; Ding, X.; Svarovskaia, E.; Symonds, W. T.; Hindes, R. G.; Berrey, M. M. Nucleotide polymerase inhibitor sofosbuvir plus ribavirin for hepatitis C. *N. Engl. J. Med.* **2013**, *368* (1), 34−44.
(21) A similar approach was reported in: Hecker, S. J.; Reddy, K. R.; van Poelje, P. D.; Sun, Z.; Huang, W.; Varkhedkar, V.; Reddy, M. V.; Fujitaki, J. M.; Olsen, D. B.; Koeplinger, K. A.; Boyer, S. H.; Linemeyer, D. L.; MacCoss, M.; Erion, M. D. Liver-Targeted Prodrugs of 2′-*C*-Methyladenosine for Therapy of Hepatitis C Virus Infection. *J. Med. Chem.* **2007**, *50*, 3891−3896.
(22) For our early work on this convergent synthesis, see: Metobo, S. E.; Xu, J.; Saunders, O. L.; Butler, T.; Aktoudianakis, E.; Cho, A.; Kim, C. U. Practical synthesis of 1'-substituted Tubercidin *C*-nucleoside analogs. *Tetrahedron Lett.* **2012**, *53*, 484.
(23) Gardelli, C.; Attenni, B.; Donghi, M.; Meppen, M.; Pacini, B.; Harper, S.; Di Marco, A.; Fiore, F.; Giuliano, C.; Pucci, V.; Laufer, R.; Gennari, N.; Marcucci, I.; Leone, J. F.; Olsen, D. B.; MacCoss, M.; Rowley, M.; Narjes, F. Phosphoramidate Prodrugs of 2′-*C*-Methylcytidine for Therapy of Hepatitis C Virus Infection. *J. Med. Chem.* **2009**, *52*, 5394−5407.
(24) Independent from our work, a similar approach was recently published Ross, B. S.; Reddy, P. G.; Zhang, H.-R.; Rachakonda, S.; Sofia, M. S. Synthesis of Diastereomerically Pure Nucleotide Phosphoramidates. *J. Org. Chem.* **2011**, *76*, 8311−8319.